1973

Models and Cost Functionals for Optimal Automatic-Generation Controllers.

Thomas William Reddoch
Louisiana State University and Agricultural & Mechanical College

73-27,865

REDDOCH, Thomas William, 1945-
MODELS AND COST FUNCTIONALS FOR OPTIMAL AUTOMATIC GENERATION CONTROLLERS.

The Louisiana State University and Agricultural and Mechanical College, Ph.D., 1973
Engineering, electrical

University Microfilms, A XEROX Company, Ann Arbor, Michigan

MODELS AND COST FUNCTIONALS FOR OPTIMAL AUTOMATIC GENERATION CONTROLLERS

A Dissertation

Submitted to the Graduate Faculty of the
Louisiana State University and
Agricultural and Mechanical College
in partial fulfillment of the
requirements for the degree of
Doctor of Philosophy

in

The Department of Electrical Engineering

by

Thomas William Reddoch
B. S., Lamar University, 1967
M. E. S., Lamar University, 1969
May, 1973

ACKNOWLEDGMENT

The author wishes to express his graditude to Louisiana State University for providing an opportunity which has enhanced his growth as a human being; to the entire staff of the Department of Electrical Engineering for assistance and friendship; to Dr. P. M. Julich for his help and support; to Dr. O. T. Tan for his thoughtful attention and interest; to the Shell Foundation and Themis Contract No. F-44620-68-C-0021 which is administered by the Air Force Office of Scientific Research for financial assistance; and to the other dear and devoted friends to numerous to mention.

Special appreciation is directed to Mrs. Debra P. Blanchard and Miss Helen A. Chisholm for the typing of the manuscript and to Margaret Bruce and Ronald LaCarna for their assistance with the final manuscript.

Finally, the author is forever indebted to his mother, Evelyn Reddoch, and his father, the late Daniel M. Reddoch, Sr. for their many years of encouragement and to Dianne Reddoch for her support and devotion.

TABLE OF CONTENTS

LIST OF TABLES

LIST OF FIGURES

ABSTRACT

A comprehensive description of the automatic generation control problem is given. State variable models are formulated for the master controller algorithm design which are consistent with present-day operating policies of interconnected power systems. Procedures are developed to systematically obtain the optimal parameters of a linear feedback control which minimize a quadratic cost functional form. The controller algorithm design concepts are illustrated numerically on two and three-area interconnected systems for various performance indices and operating conditions. Finally, decomposition methods are examined in order to develope a local controller and to optimize a multi-area system via reduced computation effort.

Chapter 1

INTRODUCTION

As the demand for electrical energy has increased, utility companies have expanded their facilities at an abnormally rapid rate. The once relatively simple power systems have become intricate interconnected networks with very complex system management problems. The northeast black-out of the mid 1960's is an indication of the potential repercussions associated with a failure in this complicated system. However, this catastrophic occurrence has provided some of the impetus for the rebirth of power systems research in the academic community. Although the utility companies have had an ongoing research program, they have been criticized for not making a larger effort. It has been suggested [MEE]* that a comprehensive study of future needs be undertaken at an estimated expenditure in excess of twice the current rate.

An investigation of the applicability of system techniques such as optimal control and estimation [ATH], and Liapunov stability theory [KA1] to the power industry is underway. The subject of this study is an analysis of the application of advanced control theory to the automatic generation control (AGC) problem. More specifically, this dissertation involves the use of optimal control theory to formulate an

*References denoted by brackets are listed in the bibliography.

improved controller algorithm which reflects the basic operating policies of present-day power systems [C01]. Some work, most within the academic community, has been done in this area, however, much of it is not consistent with present-day power system policies. This study endeavors to clearly define the AGC problem and to demonstrate how advanced control theory can be used to design a controller which is compatible with industry practices.

Any discussion of the AGC problem requires an understanding of the control area concept. A control area is interpreted as a power system with a common generation control scheme. This system may consist of a portion of a utility, a single utility or a collection of utilities. The term control area is applicable to either an isolated or an interconnected system. The AGC problem is concisely defined as matching total system generation to existing load demand with the most efficient and reliable distribution among individual units of the control area.

In order to completely appreciate the AGC practices of present-day power systems, an investigation of its evolution is necessary. Prior to the interconnecting of adjoining power systems, each system functioned independent of its neighbor. This mode of operation defines an isolated system. In this arrangement a system strives to maintain its scheduled frequency and restrict internal transmission line power flows such that no line becomes overloaded, but total generation matches load demand. Hence, controllers regulate the frequency and power flows independent of one another while efficiently distributing generation among the units.

Most modern power systems in the United States are interconnected with their neighbors to increase system security and for more efficient operation. The ultimate goal is a nationwide interconnection of all control areas into one large network. A system of this scope requires changes in the operating practices of individual control areas, but each remains responsible for meeting its own load demand, doing its share of system frequency regulation, and maintaining proper power flow to the adjoining areas.

As a member of an interconnected system, a control area attempts to regulate its <u>area</u> <u>control</u> <u>error</u> (ACE), whereby it meets its obligation to the interconnection. The ACE is a linear combination of the frequency and the net interchange power deviations related by the <u>frequency</u> <u>bias</u> constant. The frequency bias determines the amount of offset in scheduled net interchange power deviation of the control area that varies proportionately to the frequency deviation and is an indication of the stiffness of the interconnection.

A basic understanding of the controller operation employed currently by industry for the AGC problem is imperative to the discussion. During normal operation a change in load demand does not necessarily command controller action. The nature of the control is primarily permissive, i.e., it reacts to an actual ACE [RO1, RO2, RO3] after certain pre-established values are attained. Much of the control is performed by the natural governing action of the area rather than by supplementary regulation. The decision for supplmentary control and its character rests with a central control computer which monitors the ACE and the economic distribution among units of the area. The

natural governing action is classified as <u>primary</u> AGC [EL1] while the permissive control is called <u>secondary</u> AGC [EL1].

Extensive studies [BEN, CO1, CN1, CN2, EL4, KIR, QUA, RO1, RO2, RO3, VAN] on secondary control have been conducted principally for classical or conventional control schemes. Other works [BOH, CAV, EL1, MI1] have used advanced control theory on the secondary control problem without directing sufficient attention to the basic operating policies of present-day power systems.

Most of the studies applying advanced control theory for the design of the automatic generation controller (AGCR) are not concerned with secondary control. These studies are exploring expanded usage of the controller in primary AGC activity. By and large, the following two new primary control functions have emerged: 1) to clear fast transients or regulate the system for every moment in time, and 2) to increase the damping constant of interconnected systems. Neither of these functions are performed by the traditional AGC controller.

At least some of the works [BOH, CAV EL1, MI1, RE1] have attempted to differentiate between primary and secondary control functions while others [CA1, CA2, EL3, EL4, RE2] have not as each has formulated a controller algorithm. This study attempts to explore these functions as well as the traditional one and combine all of these functions into one comprehensive controller algorithm. The algorithm will incorporate suggestions of the preliminary works [CA1, CA2, RE1, RE2, RE4] which have sought to include necessary constraints of present-day power system policies.

Most studies related to the application of advanced control theory to the AGC problem have devoted little effort to the selection

of the performance index. Since this is one of the most significant elements in the parameter selection process of the control scheme, it is imperative that the performance index be structured to reflect the basic operating policies of interconnected systems. Furthermore, the relationship between the central control computer and the performance index is demonstrated. Preliminary studies [CA1, CA2, RE1, RE2, RE4] on performance index selection are available.

Finally, consideration is given to controller formulation for the multi-area power system where techniques from the broad topic of hierarchical, multilevel control [MES] are applicable. Applications of these techniques to power systems are found in a few works [LIA, NIC, MI2]. Only the most elementary form of multilevel studies [BUC, RE3] are examined in this study.

Chapter 2

AUTOMATIC GENERATION CONTROL

In an electrical power system an effort is continuously made to maintain the appropriate frequency and the net interchange power. A control system is required to regulate these quantities in the presence of changing load demand. The operation of this system is known as AGC. A thorough and complete description of the AGC problem is presented herein. Various uses and limitations of the AGCR are examined in detail to illustrate its effectiveness and to show how a new design might expand its usefulness. Suitable models for the control area are developed which are consistent with the small disturbances normally managed by the AGCR.

2.1. Physical Process

The traditional function of the AGCR, i.e., to accommodate small variations in real power demand, is explored. The feasibility of using the AGCR to clear fast transients or regulate the ACE for every moment in time and to improve system stability margin is considered. These latter two functions have been suggested following preliminary investigations of realizing the AGCR via some advanced control strategy. There appears to be sufficient evidence that an AGCR realized with complete state variable feedback as opposed to the conventional selected state variable feedback strategy could perform these functions admirably.

2.1-1. Traditional AGC

The AGC concept has been developed as a method to assist the control area in fulfilling its obligation to the interconnected system. Fundamentally, AGC is to match area generation to area load demand in the most economical way and to maintain power flow committments to the adjoining areas. The AGC objective is achieved by regulating the ACE.

In Figure 1, a simplified block diagram of a typical AGCR is shown. This controller is representative of the one used in practice in present-day power systems [RO3].

The AGCR functions are primarily performed by:

1) Master Controller - MC is the control policy for the area principally employing proportional and reset capability.
2) Error Adaptive Control Computer - EACC is a decision making computer which is responsible for determining the probability that control action is needed for regulating the ACE. Moreover, it makes adjustments in the MC gain, determines the frequency of the control cycle, and directs economic dispatch update. EACC makes the control process adaptive.
3) Pointer Count Down Controller - PCDC determines the amount of participation of each of the generating units in the activity of the control area. Also, information is relayed to the MC to account for rate of generation change limitations and to assist in determining area control policy.

In Figure 1, two additional control functions are noted: 1) an emergency by-pass to each unit and 2) a feedforward path to accommodate scheduled generation changes. It should be noted that the control pulse

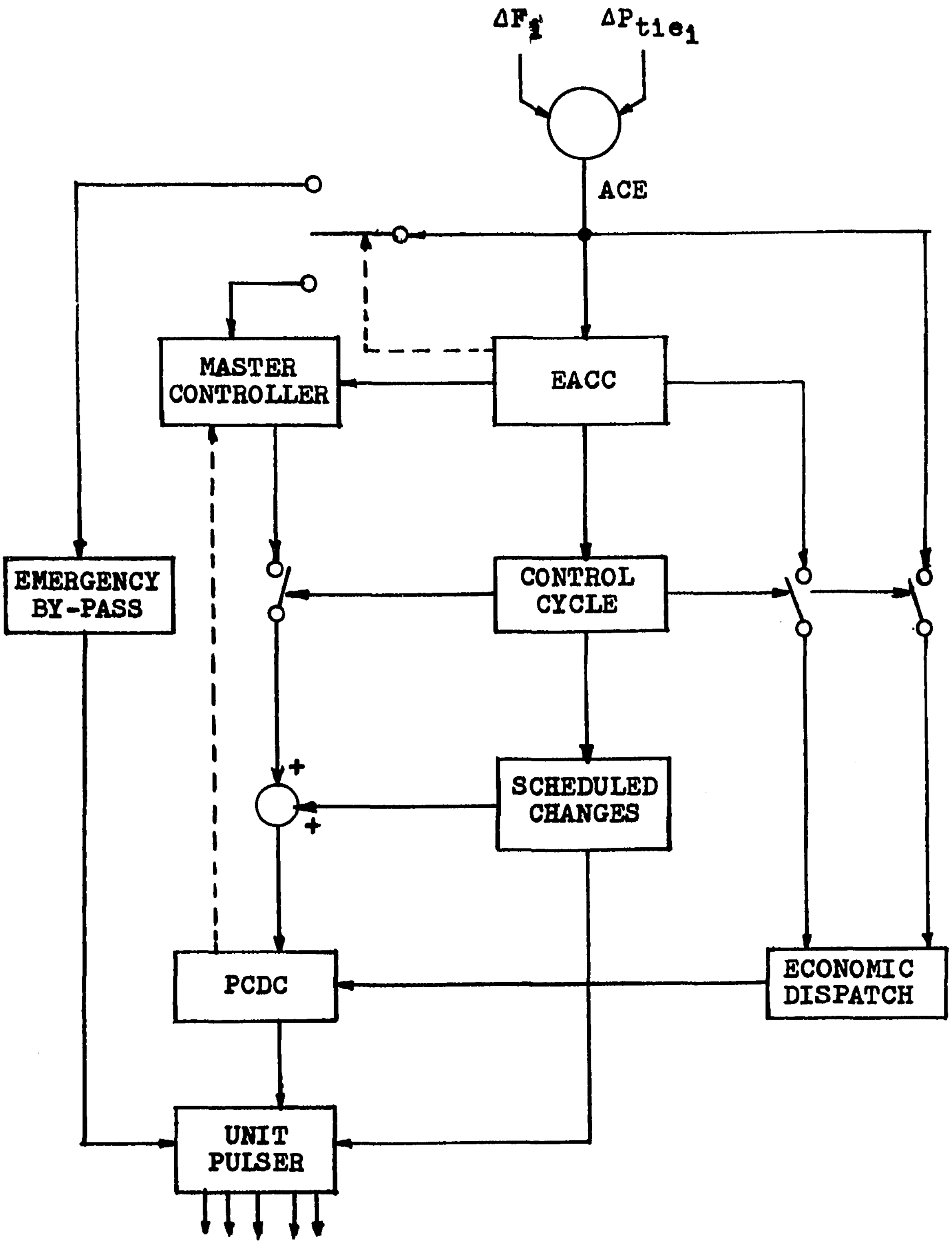

FIGURE 1. Area Automatic Generation Controller

output is for the jth unit in the control area.

In summary, control action is motivated effectively in three different ways. First, a sufficiently large or sustained deviation in the ACE will trigger the MC or emergency by-pass. Secondly, scheduled changes in generation or tie line committments are accommodated separately. Thirdly, an economic dispatch update will change allocation of generation among the units of the area.

The nature of the control process is characterized as permissive since it permits an actual ACE. A satisfactory system performance relies upon the inertia of the large interconnected system to accommodate most immediate load demand. This large system permits a sluggish control scheme via trading power flow with its neighbors.

Although the ACE represents a generation deficiency for an area, an effort is not always made to correct it. The primary objective is to reduce the ACE while minimizing those generation changes that do not make a contribution to improve system performance. From a practical point of view, it is not feasible to always minimize the ACE because of rate of generation change limitation, system nonlinearities such as deadband, and fruitless chasing of rapidly varying loads. In many cases it is sufficient to allow the natural governing action to regulate [RO1].

Although the control process is permissive, it is adaptive. EACC and PCDC provide information for MC update to accommodate changes in operating conditions on the system. Emergency situations and scheduled generation changes are given special attention.

In conclusion, the AGCR operates sequentially in the following manner [CO1]:

1) A load increase is absorbed immediately at the expense of a decrease in speed of the rotating machinery in the area, a borrowing of power from its neighbors, and a shedding of frequency sensitive loads.
2) Natural governing action of the generation occurs following a frequency droop.
3) Supplementary governor action via the AGCR occurs in the area in which the load demand changes.
4) An economic reevaluation occurs during and following the absorption of the load change.

A complete analysis and redesign of the entire AGCR is not the intent of this study. Rather, an effort is made to improve the design of the MC and to demonstrate how EACC and PCDC interact in the selection of the control scheme. The decision making processes used by EACC and PCDC to arrive at the desired control policy are not considered. A simplification of Figure 1 is shown in Figure 2 which emphasizes the MC, EACC, and PCDC as well as how they determine area control functions.

From Figure 2, a concise description of the operation of a control area is obtained. Following a load change in control area A_i, there is a deviation in the area frequency ΔF_i and the area net interchange ΔP_{tie_i}. These quantities are combined with the tie line bias constant B_i to form the ACE_i, i.e.,

$$ACE_i = B_i \cdot \Delta F_i + \Delta P_{tie_i}.$$

Now EACC examines the character of the ACE and decides whether or not control action is required. Both EACC and PCDC supply necessary

information to the MC to determine the nature of the control action if indeed it is needed.

Next attention must be devoted to the required capabilities of the MC. There are two basic requirements: 1) regulate the ACE and 2) actuate during both normal and abnormal mode of area operation in accordance with the basic operating policies of interconnected power systems [CO1].

Obviously, if the controller is to regulate the ACE, then it must have some type of proportional action to prohibit large fluctuations. This is referred to as primary control [EL1] since it reacts quickly. Proportional control is similar to the natural governing action, except the supplementary control is not permitted to act at every moment in time. Clearly, the controller must contain reset action so that step load changes can be absorbed by the area. This is a much slower activity and thus it is referred to as secondary control [EL1].

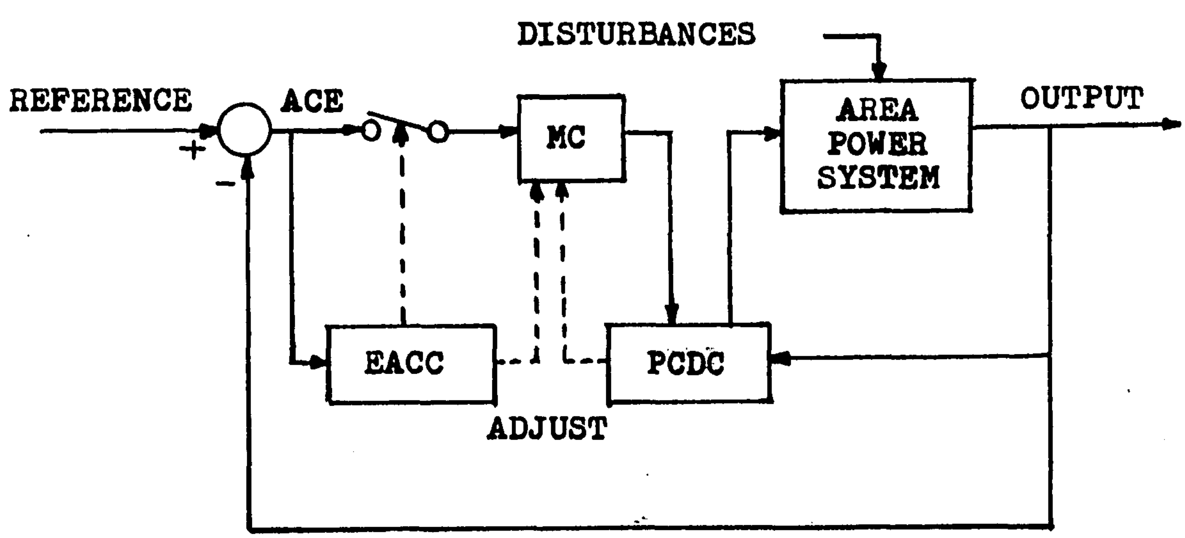

FIGURE 2. General Control Process

In an n-area interconnected system, each control area has its own responsibilities. In order to fulfill its obligations, an area must strive to maintain its ACE at zero in the steady state. If an area is unable to absorb its load increases, its ACE is not zero in the steady state; however all remaining areas have zero ACEs in the steady state.

Therefore, if area A_j experiences an increase in load, then the normal operation mode implies that A_j is capable of absorbing the load or

$$ACE_i = 0 \Rightarrow \Delta F_i = \Delta P_{tie_i} = 0 \quad \text{for } i = 1, 2, \cdots, n.$$

The abnormal mode defines operation in which A_j is not capable of absorbing all or a portion of an increase in load demand. Therefore,

$$ACE_j \neq 0 \Rightarrow \Delta F_j \neq 0, \quad \Delta P_{tie_j} \neq 0$$

$$ACE_i = 0 \Rightarrow \Delta F_i \neq 0, \quad \Delta P_{tie_i} \neq 0 \quad \text{for } i \neq j, \quad i = 1, 2, \cdots, n.$$

In summary, the MC must not only accommodate its own load, but it must be compatible with its neighbors regulatory efforts. The offset in frequency and net interchange power during the abnormal mode of operation is determined by the tie line bias constant. These offsets are temporary for it is assumed that the area in need will correct the errors by adding another generating unit, by contracting additional power from another control area or by load shedding.

The MC consists of both proportional and reset action. A conventional realization of the controller uses frequency, net interchange power, and/or the ACE since these quantities are directly

available in the output of the system.

2.1-2. Expanded Usage of the AGCR

The AGCR currently used within the power industry has a slow response capability. If a controller is developed with a quick response capability without unnecessarily moving generation, then an effort to regulate the ACE at all time may be feasible. A complete state variable feedback controller (SVC), i.e., one constructed of all the state variables used to describe the control area, is a feasible realization. Since this controller is only concerned with small load variations, linear system techniques are applicable. Extensive methodology [ATH] is available for linear optimal feedback control design with an integral square performance criterion.

Although the controller is developed with a quick response capability, it must be adaptive in order to retain the traditional operating policies. The response properties of a SVC are altered via performance index selection. Therefore, the response characteristics of the SVC may be systematically changed by using EACC and PCDC to provide information for selecting the performance index. For a specific performance index, parameter optimization procedures [ATH] exist for deriving the best control policy. This is preferable to the classical one of trial and error.

Two requirements remain. First, the availability of all the state variables is implied. This goal may be achieved via some state estimation algorithm. Secondly, the desired system transient performance must be translated into the integral square performance criterion.

As a final point of consideration, SVC increases the damping

constant of the system. Since the AGC process is concerned primarily with small load disturbances, the stability of the system is ascertained from the closed loop roots of the system. When the SVC is compared with the efforts of a conventional realization [CAV, EL1, EL3, EL4, RE4], the former is seen to improve the damping constant.

The quick response capability of the SVC makes it feasible to assist in controlling the system in the presence of large disturbances such as a line trip or a fault. Analysis of this problem involves the solution of a set of highly nonlinear equations. Therefore, it should be emphasized that the control scheme is not optimal for the large disturbance problem. Although the traditional AGCR will assist in this capacity [SC1, SC2], the SVC realization should perform much better because of its superior speed qualities.

2.2. AGC Models

Since the AGC concept is based on fulfilling the obligation of the control area, a careful definition and representation of an area and its elements is needed. In a strict sense, a load disturbance causes the various machines of the control area to operate at different speeds; however, groups of machines which are stiffly connected electrically do swing near coherency in the presence of small disturbances. A collection of stiffly connected machines with a common control policy defines a control area, the fundamental sub-portion of an interconnected system.

Although this dissertation has dwelled on control of real power and frequency (PF) of the control area, it is evident that reactive power and voltage (QV) control must also be achieved. For

small disturbances, several works [CN1, CN2, BEN, EL1] have demonstrated that PF and QV controls operate independent of one another. PF control is usually achieved through signals introduced into the governor whereas QV control is performed via the exciter. Other studies [HAN, SC3] have shown that the QV control can be effectively used to assist the PF channel. This is the only aspect of the QV control given any attention in this study.

The dynamics of the PF channel are of principal concern in this study. The four basic elements of a control area are the dynamics of the rotating machinery, (inertia and damping), the governor, the prime mover, and the transmission network for interchange power. Figure 3 illustrates the interconnection of these elements. The models chosen for the various elements are consistent with the objectives of this study.

2.2-1. Rotating Machinery Dynamics

The dynamics of the rotating machinery are characterized by the power equilibrium equation

$$\Delta P_i = \frac{dW_{ki}}{dt} + D_i \Delta F_i \tag{2.1}$$

where ΔP_i is the net incremental area power, W_{ki} is the total kinetic energy of the area, and D_i is the effective frequency sensitive damping. Obstensibly, the net area power deviation is absorbed via a time rate of change of the total kinetic energy of the rotating machinery and by frequency sensitive elements.

The net incremental area power consists of three parts: 1) ΔP_{gi}, the incremental power output from the prime mover, 2) ΔP_{Di},

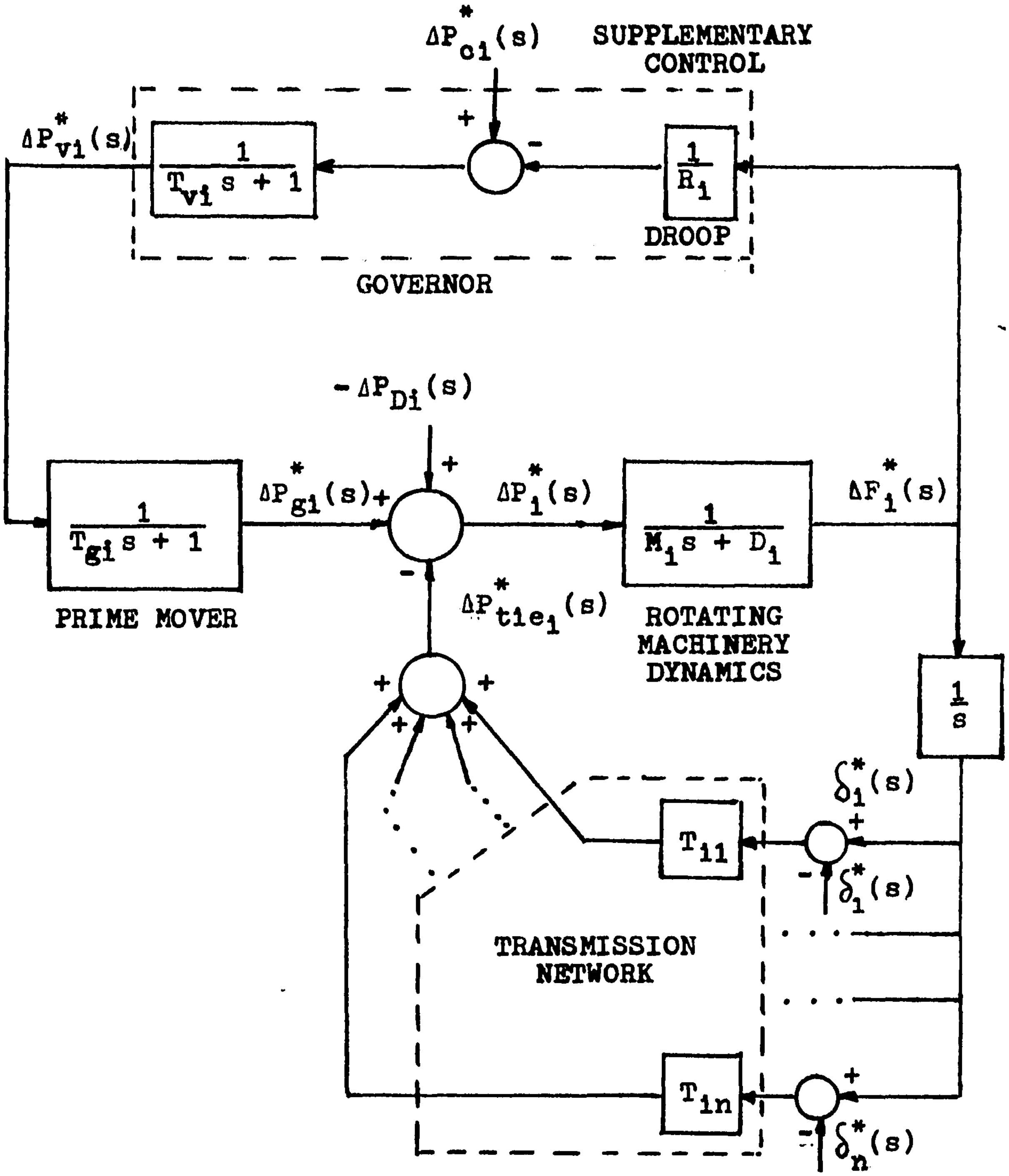

FIGURE 3. Incremental Model of the ith Control Area

the load deviation, and 3) ΔP_{tie_i}, the net power interchange deviation, where

$$\Delta P_i = \Delta P_{gi} - \Delta P_{Di} - \Delta P_{tie_i} .$$

It has been shown [EL2] that the time rate of change of the total kinetic energy can be related to the frequency deviation, ΔF_i. Since the total kinetic energy W_{ki} is proportional to the square of the frequency, then for some nominal frequency, F_O the total kinetic energy is W_{Oi}. Therefore,

$$W_{ki} = \left[\frac{F_i}{F_O}\right]^2 W_{Oi} . \tag{2.2}$$

Assume a first order expression for the variation in frequency

$$F_i = F_O + \Delta F_i . \tag{2.3}$$

Upon substitution of equation (2.3) into equation (2.2)

$$W_{ki} = \left[\frac{F_O + \Delta F_i}{F_O}\right]^2 W_{Oi} = \frac{F_O^2 + 2\Delta F_i F_O + \Delta F_i^2}{F_O^2} W_{Oi} . \tag{2.4}$$

For ΔF_i small, equation (2.4) becomes

$$W_{ki} \approx \left[1 + \frac{2\Delta F_i}{F_O}\right] W_{Oi} .$$

Therefore,

$$\frac{dW_{ki}}{dt} = \frac{2W_{Oi}}{F_O} \frac{d\Delta F_i}{dt} .$$

Since per-unit quantities are generally used, ΔP_i and D_i are expressed in per-unit of the total rated power of the area, P_{ri}. The

total kinetic energy of the area is conveniently related to the per-unit inertia constant H_i as

$$H_i = \frac{W_{0i}}{P_{ri}} \cdot$$

Now

$$\frac{dW_{ki}}{dt} = \frac{2H_i P_{ri}}{F_0} \frac{d\Delta F_i}{dt} = M_i \frac{d\Delta F_i}{dt}$$

where M_i is the "effective" per-unit inertia constant.

The effective area damping consists of two parts: 1) frequency sensitive load torques and 2) frequency sensitive turbine torques. Load torques introduce positive damping into the system while turbine torques create negative damping. The determination of the various components of these torques is exceedingly complex and thus it is not included here [CRA].

Summarizing equation (2.1) with incremental variables and in per-unit

$$M_i \frac{d\Delta F_i}{dt} + D_i \Delta F_i = \Delta P_{gi} - \Delta P_{Di} - \Delta P_{tie_i} \qquad (2.5)$$

or as a transfer function

$$\frac{\Delta F_i^*(s)}{\Delta P_i^*(s)} = \frac{1}{M_i s + D_i} \, .$$

2.2-2. Governor Dynamics with Droop

Fundamentally, the governor changes the prime mover input following a change in the frequency or speed of the generator. There

are basically two types, either isochronous or with speed droop. An isochronous unit maintains a constant speed at all levels of power produced by the prime mover within its maximum capacity. A governor with a speed drooping characteristic allows a frequency increase and decrease about some nominal value for some specified level of output power. The latter form is the most widely used type.

In Figure 3, an incremental model of the governor is shown. Several works [EL4, HAM] have analyzed the dynamical properties of the governor and they have shown that a single time lag is an adequate characterization.

The governor is constantly acting to reduce the frequency deviation via its droop characteristic. The amount of droop is determined by the regulation,

$$R = -\frac{\Delta F_s}{\Delta P_{gs}}$$

where ΔF_s and ΔP_{gs} are the static frequency deviation and static incremental generated power of the area without the presence of supplementary control. The supplementary control ΔP_{ci} for the area is introduced via the governor.

Finally, an incremental equation for the governor is

$$T_{vi}\frac{d\Delta P_{vi}}{dt} + \Delta P_{vi} = \Delta P_{ci} - \frac{1}{R}\Delta F_i \qquad (2.6)$$

or in transfer function form:

$$\frac{\Delta P^*_{vi}(s)}{\Delta P^*_s(s)} = \frac{1}{1 + sT_v}$$

where

$$\Delta P^*_s(s) = \Delta P^*_{ci}(s) - \frac{1}{R}\Delta F^*_i(s).$$

2.2-3. Prime Mover

The prime mover is a turbine-generator which provides the generated electrical power for the control area. The turbine converts the available energy supply to mechanical power to drive the generator. There are several different kinds of turbines, but each is controlled by a governor that manipulates a valve or gate.

The effect of the prime mover may be characterized as a change in valve position which causes a change in generated power. Under the assumption that QV control is much faster than the PF control, the voltage of the generator remains constant during PF channel transients unless the voltage is deliberately offset. Hence, the generator is represented as a gain, unity in value. A simplified transfer function [PAR] for a nonreheat turbine is a single time lag.

Therefore, the prime mover is represented by a transfer function relating the incremental valve position ΔP_{Vi} to the incremental generated power ΔP_{gi}:

$$\frac{\Delta P^*_{gi}(s)}{\Delta P^*_{Vi}(s)} = \frac{1}{1 + sT_{gi}}$$

or in equation form

$$T_{gi}\frac{d\Delta P_{gi}}{dt} + \Delta P_{gi} = \Delta P_{Vi}. \tag{2.7}$$

2.2-4. Net Interchange Power

The net interchange power for the ith area is assumed to be described by the synchronizing power equation

$$P_{tie_i} = \sum_{\substack{j=1 \\ j \neq i}}^{n} \frac{2\pi |E_i||E_j|}{X_{ij} P_{ri}} \sin(\delta_i - \delta_j)$$

where $|E_i|$ is the effective voltage magnitude of the ith area,

$|E_j|$ is the effective voltage magnitude of the jth area,

δ_i is the integral of the frequency of the ith area,

δ_j is the integral of the frequency of the jth area,

X_{ij} is the reactance of the line connecting the ith area to the jth area.

In this study an incremental net interchange power equation is needed. Therefore,

$$\Delta P_{tie_i} = \frac{\partial P_{tie_i}}{\partial |E_i|} \Delta |E_i| + \sum_{\substack{j=1 \\ j \neq i}}^{n} \frac{\partial P_{tie_i}}{\partial |E_j|} \Delta |E_j|$$

$$+ \sum_{\substack{j=1 \\ j \neq i}}^{n} \frac{\partial P_{tie_i}}{\partial (\delta_i - \delta_j)} \Delta(\delta_i - \delta_j)$$

where

$$\frac{\partial P_{tie_i}}{\partial |E_i|} = \sum_{\substack{j=1 \\ j \neq i}}^{n} \frac{2\pi |E_j|}{X_{ij} P_{ri}} \sin(\delta_i - \delta_j),$$

$$\frac{\partial P_{tie_i}}{\partial |E_j|} = \frac{2\pi |E_i|}{X_{ij} P_{ri}} \sin (\delta_i - \delta_j),$$

$$\frac{\partial P_{tie_i}}{\partial (\delta_i - \delta_j)} = \frac{2\pi |E_i| |E_j|}{X_{ij} P_{ri}} \cos (\delta_i - \delta_j).$$

Now evaluate the partial derivatives for some nominal operating point and define the following

$$\frac{\partial P_{tie_i}}{\partial |E_i|} = \sum_{\substack{j=1 \\ j \neq i}}^{n} \frac{2\pi |E_j|}{X_{ij} P_{ri}} \sin (\delta_i - \delta_j) \equiv T_i$$

$$\frac{\partial P_{tie_i}}{\partial |E_j|} = \frac{2\pi |E_i|}{X_{ij} P_{ri}} \sin (\delta_i - \delta_j) \equiv T_j \text{ for } j \neq i \tag{2.8}$$

$$\frac{\partial P_{tie_i}}{\partial (\delta_i - \delta_j)} = \frac{2\pi |E_i| |E_j|}{X_{ij} P_{ri}} \cos (\delta_i - \delta_j) \equiv T_{ij} \text{ for } j \neq i.$$

The incremental net interchange equation becomes

$$\Delta P_{tie_i} = T_i \Delta |E_i| + \sum_{\substack{j=1 \\ j \neq i}}^{n} T_j \Delta |E_j| + \sum_{\substack{j=1 \\ j \neq i}}^{n} T_{ij} \Delta (\delta_i - \delta_j). \tag{2.9}$$

Equation (2.9) is a general expression for the incremental net interchange power caused by voltage and angular effects. Since the angle is the integral of the frequency deviation, the angular part of equation (2.9) is created by the PF channel. The voltage terms in equation (2.9) are caused by the QV channel, and thus illustrates how QV control can affect the PF channel.

Since the QV transients are much faster than those of the PF channel, no voltage change is generally assumed in PF analysis.

Therefore, equation (2.9) simplifies to

$$\Delta P_{tie_i} = \sum_{\substack{j=1 \\ j \neq i}}^{n} T_{ij} \Delta(\delta_i - \delta_j). \tag{2.10}$$

CHAPTER 3

COMPONENTS OF THE ANALYSIS

3.1. Optimization Mathematics

Techniques [ATH] for the design of an optimal linear feedback regulator are quite well known. These methods are based on a linear set of state equations and a quadratic performance functional as inputs to a Ricatti differential equation which provides the optimal parameters for the feedback control. Implicit to the realization is the availability of all state variables.

The widespread usage of these optimization techniques has been devoted to the design of proportional controllers. Frequently, a regulator with integral action is sought in order to achieve desirable steady state performance properties in the presence of various kinds of disturbances. The addition of integration may destroy such properties as controllability and observability which may be detrimental to the optimization routines. Hence, a careful examination of the procedures is necessary.

3.1-1. Proportional Optimal Control

The basic linear time invariant regulator problem is characterized by the equations

$$\begin{aligned} \dot{x}(t) &= Ax(t) + Bu(t) \\ y(t) &= Cx(t) \end{aligned} \tag{3.1}$$

where $x(t)$ is an n-state vector,

A is an nxn-system matrix,

$u(t)$ is an m-control vector,

B is an nxm-control matrix,

$y(t)$ is an 1-output vector,

C is an lxn-output matrix.

An infinite time quadratic cost functional is defined as

$$J = \frac{1}{2} \int_0^\infty \left[x^T(t)Qx(t) + u^T(t)Ru(t) \right] dt$$

where Q is a positive semidefinite nxn-matrix and R is a positive definite mxm-matrix. Given the hypothesis of controllability, it is well known [KA2] that a unique optimal control exists as

$$u^*(t) = -R^{-1}B^T Kx(t)$$

where K is an unique symmetric positive definite nxn-matrix solution to the matrix algebraic Ricatti equation

$$KA + A^T K - KBR^{-1}B^T K + Q = 0.$$

In general, the control will contain all of the state variables.

3.1-2. Proportional Plus Integral Optimal Control

In classical control theory, reset or integral control is used to eliminate steady state errors in the output of a system. The standard optimal control problem provides a scheme with proportional action since only initial condition disturbances are assumed, thus it cannot accommodate sustained external disturbances with zero steady state error in the output. However, a new problem formulation can provide reset capability

by augmenting the original system equations with an appropriate set of integral expressions.

The stable closed loop system of equation (3.1),

$$\dot{x}(t) = Dx(t) + d$$

where D is a constant nxn-matrix and is invertible and d is a constant n-vector, will have a steady state value of

$$x_{ss} = -D^{-1}d.$$

Generally, x_{ss} is nonzero provided d is nonzero.

If x(t) is augmented with a set of integral equations, z(t) of order r, then a new system is formulated as

$$\begin{bmatrix} \dot{x}(t) \\ \hline \dot{z}(t) \end{bmatrix} = \left[\begin{array}{c|c} D_1 & 0 \\ \hline D_2 & 0 \end{array}\right] \begin{bmatrix} x(t) \\ \hline z(t) \end{bmatrix} + \begin{bmatrix} d \\ \hline 0 \end{bmatrix}$$

where D_1 and D_2 are nxn-matrices, respectively or more succinctly as

$$\dot{\hat{x}}(t) = \hat{D}\hat{x}(t) + \hat{d}. \tag{3.2}$$

The steady state error for the new system is

$$\hat{x}_{ss} = -\hat{D}^{-1}\hat{d}.$$

Now, if $\hat{D}^{-1}$ is expressed in partioned form as

$$\hat{D}^{-1} = \left[\begin{array}{c|c} Z_{11} & Z_{12} \\ \hline Z_{21} & Z_{22} \end{array}\right]$$

where Z_{11}, Z_{12}, Z_{21}, and Z_{22} are nxn, nxr, rxn, and rxr matrices, respectively; then it is evident that

$$x_{ss} = -Z_{11}d. \tag{3.3}$$

A sufficient condition for zero elements in x_{ss} is that corresponding rows of Z_{11} are zero. The sufficient condition on Z_{11} has been shown [P01], but it is repeated in part to demonstrate an understanding of the use of integral action in optimal feedback control design.

First, a set of integral equations of order $r \leq m$ [P02] defined on the original set of variables, equation (3.1),

$$\dot{z}(t) = Tx(t) \tag{3.4}$$

where T is an rxn-matrix with its rows the same as the first r rows of a nxn identity matrix. Clearly, the elements of x(t) can be arranged to fulfill this requirement.

Now, equation (3.1) is augmented with equation (3.4) yielding

$$\begin{aligned} \begin{bmatrix} \dot{x}(t) \\ \hline \dot{z}(t) \end{bmatrix} &= \left[\begin{array}{c|c} A & 0 \\ \hline T & 0 \end{array}\right] \begin{bmatrix} x(t) \\ \hline z(t) \end{bmatrix} + \begin{bmatrix} B \\ \hline 0 \end{bmatrix} u(t) \\ y(t) &= \left[\begin{array}{c|c} C & 0 \end{array}\right] \begin{bmatrix} x(t) \\ \hline z(t) \end{bmatrix} \end{aligned} \tag{3.5}$$

or more concisely

$$\begin{aligned} \dot{\hat{x}}(t) &= \hat{A}\hat{x}(t) + \hat{B}u(t) \\ y(t) &= \hat{C}\hat{x}(t), \end{aligned} \tag{3.6}$$

where $\hat{x}(t)$ is an augmented (n+r)-state vector,

$\hat{A}$ is an augmented (n+r)x(n+r)-system matrix,

u(t) is the original m-control vector,

$\hat{B}$ is an augmented (n+r)xm-control matrix,

y(t) is the original l-output vector,

$\hat{C}$ is an augmented lx(n+r)-output matrix.

As before, a control for equation (3.5) is desired which will minimize the performance functional

$$\hat{J} = \frac{1}{2} \int_0^\infty [\hat{x}^T(t)\hat{Q}\hat{x}(t) + u^T(t)Ru(t)]\, dt$$

where $\hat{Q}$ is a positive semidefinite constant (n+r)x(n+r)-matrix defined as

$$\hat{Q} = \left[\begin{array}{c|c} Q & 0 \\ \hline 0 & P \end{array}\right] \tag{3.7}$$

with P as a positive definite rxr-matrix. The control that minimizes $\hat{J}$ is

$$u^*(t) = -R^{-1}\hat{B}^T\hat{K}\hat{x}(t) \tag{3.8}$$

where $\hat{K}$ is the symmetric positive definite (n+r)x(n+r)-matrix solution to the matrix Ricatti algebraic equation

$$\hat{A}^T\hat{K} + \hat{K}\hat{A} - \hat{K}\hat{B}R^{-1}\hat{B}^T\hat{K} + \hat{Q} = 0 \tag{3.9}$$

provided the pair $(\hat{A},\hat{B})$ is controllable [KA2].

Careful consideration of the controllability condition is imperative because the addition of integration to the controllable pair (A,B) of equation (3.1) may cause the augmented pair $(\hat{A},\hat{B})$ of equation (3.6) to be uncontrollable [PO2]. However, it has been shown [PO3] that provided the pair (A,B) is controllable, then the pair $(\hat{A},\hat{B})$ is controllable if:

1) For a nonsingular A the rank of $TA^{-1}B$ is r

2) For a singular A the rank of $T(A + BF)^{-1}$ is r where F is any matrix which makes (A + BF) nonsingular.

The relationship between the control, equation (3.8), and the partitioned system of equation (3.5) is obtained by partitioning

$$\hat{K} = \begin{bmatrix} \hat{K}_1 & \hat{K}_2 \\ \hat{K}_2^T & \hat{K}_3 \end{bmatrix} \tag{3.10}$$

where $\hat{K}_1$, $\hat{K}_2$, and $\hat{K}_3$ are of the dimensions nxn, nxr, and rxr respectively. Then equations (3.5), (3.7), (3.8), and (3.10) are substituted into equation (3.9) producing three separate equations

$$\begin{gathered} (A^T\hat{K}_1 + T^T\hat{K}_2^T) + (\hat{K}_1A + \hat{K}_2T) - \hat{K}_1BR^{-1}B^T\hat{K}_1 + Q = 0 \\ (A^T\hat{K}_2 + T^T\hat{K}_3) - \hat{K}_1BR^{-1}B^T\hat{K}_2 = 0 \\ \hat{K}_2^TBR^{-1}B^T\hat{K}_2 - P = 0. \end{gathered} \tag{3.11}$$

Now, if equation (3.10) and expressions for $\hat{B}$ and $\hat{x}(t)$ are substituted into equation (3.8), then

$$u^*(t) = -R^{-1}B^T \; [\hat{K}_1x(t) + \hat{K}_2z(t)]. \tag{3.12}$$

After substituting equation (3.12) into equation (3.5), the closed loop system matrix is expressed as

$$\hat{D} = \begin{bmatrix} A - BR^{-1}B^T\hat{K}_1 & BR^{-1}B^T\hat{K}_2 \\ T & 0 \end{bmatrix}$$

In order to force the appropriate elements of x_{ss} in equation (3.3) to zero, then from

$$\hat{D}\,\hat{D}^{-1} = I$$

it is found that

$$T Z_{11} = 0. \tag{3.13}$$

Since the rows of T are the same as the first r rows of a nxn unit matrix, then the first r rows of Z_{11} must be zero. Hence, reset action is achieved.

Sometimes, it is desirable to regulate the steady state output to zero rather than individual states; i.e., from equations (3.1) and (3.3)

$$y_{ss} = - CZ_{11}d$$

where Z_{11} is dimensioned nx1 for this case. Choose

$$T = C$$

thus from equation (3.13)

$$CZ_{11} = 0$$

hence

$$y_{ss} = 0.$$

From this analysis, four observations are made. First, the above formulation will give an optimal control scheme with desirable steady state characteristics. Secondly, the scheme is an optimal linear feedback control in the absence of external disturbances. Thirdly, the integral states will not appear in the control scheme unless these states are weighted in the cost functional; i.e., P in equation (3.11) must be positive definite. Finally, it is seen in equation (3.11) that the integral gains are determined independently of the proportional ones but the converse is not true.

3.2 . State Variable Model

In order to apply the concepts of optimal control theory to the AGC problem, the properties both physical and operational must be translated into an appropriate state variable representation.

3.2-1. State Variable Model--PF Dynamics

The physical characteristics assuming that the PF and QV effects are separable are recalled from equations (2.5), (2.6), (2.7), and (2.10) and restated as

$$M_i \frac{d\Delta F_i}{dt} + D_i \Delta F_i = \Delta P_{gi} - \Delta P_{Di} - \Delta P_{tie_i} \tag{3.14}$$

$$T_{Vi} \frac{d\Delta P_{Vi}}{dt} + \Delta P_{Vi} = \Delta P_{ci} - \frac{1}{R_i} \Delta F_i \tag{3.15}$$

$$T_{gi} \frac{d\Delta P_{gi}}{dt} + \Delta P_{gi} = \Delta P_{Vi} \tag{3.16}$$

$$\Delta P_{tie_i} = \sum_{\substack{j=1 \\ j \neq i}}^{n} \Delta P_{ij} = \sum_{\substack{j=1 \\ j \neq i}}^{n} T_{ij} \, \Delta(\delta_i - \delta_j). \tag{3.17}$$

The basic operating policy of interconnected systems [CO1], i.e., a zero steady state ACE in the presence of a step increase in load demand, must be translated into a mathematical relation. This steady state characteristic is achieved by providing the controller with the integral of the ACE (defined IACE). Hence a new model equation is

$$\dot{IACE} = B_i \cdot \Delta F_i + \Delta P_{tie_i} \tag{3.18}$$

Several earlier studies [CAV, EL1, EL3] have failed to reflect this property.

Now, equations (3.14) - (3.18) are converted into a state variable representation as a system of first order differential equations. Clearly, ΔF_i, ΔP_{gi}, and ΔP_{Vi} are fundamental choices for state variables.

In this study and others [E11, E14, RE1, RE3], at least one tie line flow ΔP_{ij} emanating from the area is defined as a state variable rather than the angles as state variables [E12, E13] or characterizing ΔP_{ij} as a disturbance input. The net interchange power is then constructed from the individual tie line flow state variables. Finally, the $IACE_i$ is chosen as the last variable for the description of the ith area.

The following notation is adopted to describe the ith area:

$$\begin{bmatrix} \Delta F_i \\ \Delta P_{g i} \\ \Delta P_{V i} \\ \Delta P_{i j} \\ IACE_i \end{bmatrix} \equiv \begin{bmatrix} x_1 \\ x_2 \\ x_3 \\ x_4 \\ x_5 \end{bmatrix}_i \equiv \qquad \begin{array}{l} \Delta P_{c i} = U_i \\ \\ \Delta P_{D i} = V_i . \end{array}$$

Therefore the matrix equation of an n-area interconnected system is

$$\begin{bmatrix} x_1 \\ x_2 \\ x_3 \\ x_4 \\ \hline \vdots \\ \hline x_{4n} \\ \hline \vdots \end{bmatrix} = \left[\begin{array}{ccccc|c} -\frac{D}{M_1} & \frac{1}{M_1} & 0 & \frac{1}{M_1} & 0 & \cdots \\ 0 & -\frac{1}{T_{g1}} & \frac{1}{T_{g1}} & 0 & 0 & \cdots \\ -\frac{1}{T_{V1} R_1} & 0 & -\frac{1}{T_{V1}} & 0 & 0 & \cdots \\ T_{12} & 0 & 0 & 0 & -T_{12} & \cdots \\ \hline \vdots & & \vdots & \vdots & & \vdots \\ \hline B_1 & 0 & 0 & 1 & 0 & \cdots \\ \hline \vdots & & \vdots & \vdots & & \cdots \end{array}\right] \begin{bmatrix} x_1 \\ x_2 \\ x_3 \\ x_4 \\ \hline \vdots \\ \hline x_{4n} \\ \hline \vdots \end{bmatrix}$$

$$+ \left[\begin{array}{c|c} 0 & \cdots \\ 0 & \\ \frac{1}{T_{V1}} & \cdots \\ 0 & \cdots \\ \hline \vdots & \vdots \\ \hline 0 & \cdots \\ \hline \vdots & \vdots \end{array}\right] \begin{bmatrix} u_1 \\ \hline \vdots \end{bmatrix} + \left[\begin{array}{c|c} \frac{1}{M_2} & \cdots \\ 0 & \\ 0 & \cdots \\ 0 & \cdots \\ \hline \vdots & \vdots \\ \hline 0 & \cdots \\ \hline \vdots & \vdots \end{array}\right] \begin{bmatrix} v_1 \\ \hline \vdots \end{bmatrix} . \tag{3.19}$$

The output is defined in two different ways. First, an output that consists of the measurable variables, i.e., the frequency and interchange power deviations, is considered. Hence,

$$y_m = \begin{bmatrix} y_{m1} \\ y_{m2} \\ \hdashline \vdots \end{bmatrix} = \left[\begin{array}{cccc:c} 1 & 0 & 0 & 0 & \cdots \\ 0 & 0 & 0 & 1 & \cdots \\ \hdashline \vdots & \vdots & & & \vdots \end{array}\right] [X]$$

A second output consists of those quantities that are to be regulated, i.e., the ACEs. Therefore

$$y_c = \begin{bmatrix} y_{c1} \\ \hdashline \vdots \end{bmatrix} = \left[\begin{array}{cccc:c} B & 0 & 0 & 1 & \cdots \\ \hdashline \vdots & \vdots & & \vdots & \vdots \end{array}\right] [X]$$

A complete set of equations in standard form have been presented for a control area with the physical variables segregated from the integral ones. It is significant to note that the physical variables end on number 4n-1. The reason is that only n-1 tie line power flow state variables are needed to characterize an n-area interconnected system. Such cases as interconnected areas with different rated powers and multiple interconnections between areas are considered in detail as needed.

<u>3.2-2. State Variable Model -- QV Dynamics</u>

Generally, it has been assumed that the QV control operates independently of the PF control. In equation (2.9), it is shown that voltage variation can effect the net interchange power deviation, hence the QV control influences the PF dynamics. This is important because several works [HAN, SC3] have shown that the voltage variation is effective in improving the system damping. In order to incorporate these effects into the state model, a slight reformulation is needed.

Voltage variation, $\Delta|E_i|$, affects both the interchange power as seen from equation (2.9) and the effective load in each area [COL] by an amount $(\partial P_{Di}/\partial|E_i|)\ \Delta|E_i|$. The voltage variation which is produced by the exciter in effective zero time is one of the control inputs to the PF channel. Therefore the reformulation is restricted to changing the B matrix, the number of controls, the R matrix of the performance index, and the definition of the ACE.

The only equation affected by the voltage variation is that of $\Delta\dot{F}_i$ since both the net interchange power and the load enter this equation. It should be noted that the $\dot{IACE}_i$ equation is not affected because only that part of the net interchange power produced by the angle change is considered as a part of the ACE. Therefore, the power flow produced by the intentional offset of the voltage is not considered as part of the ACE.

Hence, the new B matrix is

$$B = \begin{bmatrix} 0 & 0 & \cdots & -\frac{1}{M}\left[\frac{\partial P_{D1}}{\partial|E_1|} + T_1\right] & -\frac{1}{M_1}T_2 & \cdots \\ 0 & 0 & & 0 & 0 & \\ \frac{1}{T_{V_1}} & 0 & \cdots & 0 & 0 & \cdots \\ 0 & 0 & & 0 & 0 & \\ 0 & 0 & \cdots & -\frac{1}{M_2}T_2 & -\frac{1}{M_2}\left[\frac{\partial P_{D2}}{\partial|E_2|} + T_2\right] & \cdots \\ \vdots & \vdots & & \vdots & & \vdots \end{bmatrix} \tag{3.20}$$

and the control is

$$U = [\Delta P_{c1} \quad \Delta P_{c2} \quad \cdots \quad \Delta|E_1| \quad \Delta|E_2| \quad \cdots]$$

with an appropriate increase in the order of R.

Special attention is directed at the entries in the new B matrix.

From equation (2.8) it is seen that T_i can be either positive or negative with the outcome dependent upon the nominal state of the angles of each area.

3.3. Performance Index as a Quadratic Functional

In most studies, little attention has been devoted to the selection of the performance indices. This single fact has led to much of the criticism of optimal controller design since the various performance functionals have not adequately represented the desirable operating policies. The familiar integral square error (ISE) measure is used as the performance index. Much effort is needed to devise a performance index which reflects the basic operating policies, includes some system limitations, and is easily modified to accommodate changing operating conditions in the system.

Several earlier works [CA1, RE3, RO1, RO2] indicate that two necessary elements for the performance index are the ACE_i and $IACE_i$ Obviously, the ACE_i is included to reflect basic operating policy and to insure small fluctuations in the ACE_i. This choice does lead to larger frequency and power swings, but at an acceptable level in exchange for better ACE_i characteristics. The $IACE_i$ is included to minimize area supplementary control activity [RO1] and to insure the appearance of the $IACE_i$ in the control scheme (see equation (3.11)).

Physically, there are rate of generation change (RGC) limitations for the prime mover. This is not reflected in the linear model, however the responsibility of restricting excessive RGC remains. The RGC $\Delta\dot{P}_{gi}$ is limited by including it in the performance index as a linear combination of the governor and prime mover variables as in equation (3.16).

Finally, the control ΔP_{c_i} must be included to satisfy equation (3.11). This addition reduces the control effort and determines in part the response characteristics of the controller. The relative weighting between the control and the states is the most important factor.

Therefore, the performance index for an n-area interconnected system is expressed in ISE as

$$J = \int_0^\infty \sum_{i=1}^{n} \left(\alpha_i \cdot ACE_i^2 + \beta_i \cdot IACE_i^2 + \gamma_i \cdot \frac{(\Delta P_{V_i} - \Delta P_{E_i})^2}{T_{E_i}^2} + \Delta P_{c_i}^2 \right) dt$$

corresponding to

$$Q = \left[\begin{array}{cccc|c} \alpha_1 B_1^2 & 0 & 0 & \alpha_1 B_1 & \cdots \\ 0 & \frac{\gamma_1}{T_{E1}^2} & -\frac{\gamma_1}{T_{E1}^2} & 0 & \\ & & & & \cdots \\ 0 & -\frac{\gamma_1}{T_{E1}^2} & \frac{\gamma_1}{T_{E1}^2} & 0 & \\ \alpha_1 B_1 & 0 & 0 & \alpha_1 T_{E1} & \cdots \\ \hline \vdots & \vdots & & \vdots & \cdots \end{array} \right] \qquad (3.21)$$

$$P = \begin{bmatrix} \beta_1 & 0 & \cdots \\ 0 & \beta_2 & \cdots \\ & \vdots & \vdots \end{bmatrix}, \qquad R = \begin{bmatrix} 1 & 0 & \cdots \\ 0 & 1 & \cdots \\ & \vdots & \vdots \end{bmatrix}$$

where T_{E_i} is dependent upon the number areas and the number of tie lines.

The chosen performance index consists of all the essential elements governing the operation of an interconnected power system. It should be noted that each element of the performance index has a weighting parameter except the control. In these studies it suffices to fix R as the unit matrix and to vary the weightings in Q.

Clearly, the selection of the weighting parameters will determine the nature of the response. The selection process can be made compatible with the AGCR by relegating these decisions to the EACC and the PCDC. One of the principle functions of the EACC is to control the speed of response of the area which is achieved principally by varying α_i and β_i. RGC limitations are generally determined by PCDC which is done by selecting γ_i. The RGC is affected indirectly by α_i and β_i through the speed of response of the controller. All of the parameters affect the stability.

Special attention is to be devoted to the selection of β_i because of its pronounced independent effect. From equation (3.12), the IACE gain is determined by $\hat{K}_2$ which is found independent of the other partitioned variables of equation (3.10). $\hat{K}_2$ can be determined by equation (3.11). Thus, the integral part of the control $u_I(t)$ is separated from equation (3.12) as

$$u_I(t) = -R^{-1}B^T \hat{K}_2 z(t) = K\, z(t). \tag{3.22}$$

Now, a direct relationship between the weighting parameters (i=1,2, .., n) and K_I is established for an n-area system. Recall equation (3.11)

$$\hat{K}_2^T \; BR^{-1} \; B^T \hat{K}_2 - P = 0$$

and then substitute the following matrices for an n-area system:

$$h_i \equiv \frac{1}{T_{V_i}} \qquad N \equiv 4n - 1 \qquad r = n$$

$$B = \begin{bmatrix} 0 & 0 & \\ 0 & 0 & \\ h_1 & 0 & \cdots \\ 0 & 0 & \\ 0 & 0 & \\ 0 & 0 & \\ 0 & h_2 & \cdots \\ 0 & 0 & \\ \vdots & & \cdots \end{bmatrix} \qquad \hat{K}_2 = \begin{bmatrix} k_{11} & k_{12} & k_{13} & \cdots & k_{1n} \\ k_{21} & k_{22} & k_{23} & \cdots & k_{2n} \\ \vdots & \vdots & & & \vdots \\ k_{N1} & k_{N2} & k_{N3} & \cdots & k_{Nn} \end{bmatrix}$$

$$R = \begin{bmatrix} 1 & 0 & 0 & \cdots \\ 0 & 1 & 0 & \cdots \\ 0 & 0 & 1 & \cdots \\ \vdots & & \vdots & \end{bmatrix} \qquad P = \begin{bmatrix} \beta_1 & 0 & 0 & \cdots \\ 0 & \beta_2 & 0 & \cdots \\ 0 & 0 & \beta_3 & \cdots \\ \vdots & & \vdots & \end{bmatrix}.$$

Therefore,

$$BR^{-1}B^T = \left[\begin{array}{cccc:cccc:c:c} 0 & 0 & 0 & 0 & & & & & & \\ 0 & 0 & 0 & 0 & & 0 & & & 0 & \cdots \\ 0 & 0 & h_1^2 & 0 & & & & & & \\ 0 & 0 & 0 & 0 & & & & & & \\ \hdashline & & & & 0 & 0 & 0 & 0 & & \\ & 0 & & & 0 & 0 & 0 & 0 & 0 & \cdots \\ & & & & 0 & 0 & h_2^2 & 0 & & \\ & & & & 0 & 0 & 0 & 0 & & \\ \hdashline & \vdots & & & & \vdots & & & \ddots & \cdots \end{array}\right] = R_B$$

$$e \equiv 4i - 1$$

$$\hat{K}_2^T R_B \hat{K}_2 = \begin{bmatrix} \sum_{i=1}^{n} h_i^2 k_{e1}^2 & \sum_{i=1}^{n} h_i^2 k_{e1} k_{e2} & \cdots \\ \sum_{i=1}^{n} h_i^2 k_{e1} k_{e2} & \sum_{i=1}^{n} h_i^2 k_{e2}^2 & \cdots \\ \vdots & \vdots & \end{bmatrix}.$$

Thus with

$$\hat{K}_2^T \; R_\beta \; \hat{K}_2 = P$$

then

$$\sum_{i=1}^{n} h_i^2 \; k_{ej}^2 = \beta_j \qquad \text{for } j=1,2, \ldots n$$

$$\sum_{i=1}^{n} h_i^2 \; k_{es} \; k_{et} = 0 \qquad \text{for } s,t=1,2, \ldots n \;\; \ni \; s \neq t.$$

One solution to this system of equations is

$$k_{es} = 0 \qquad \text{for } i,s=1,2,\ldots. \; n \quad s \neq i$$

$$k_{es} = \sqrt{\beta_i} \qquad \text{for } i,s=1,2, \ldots n \quad s=i.$$

Hence,

$$\hat{K}_2 = \begin{bmatrix} k_{11} & k_{12} & \sqrt{\beta_1} & k_{14} & k_{15} & k_{16} & 0 & k_{18} & \cdots \\ k_{21} & k_{22} & 0 & k_{24} & k_{25} & k_{26} & \sqrt{\beta_2} & k_{28} & \cdots \\ & & \vdots & & \vdots & & \vdots & & \cdots \end{bmatrix}$$

Now substitute $\hat{K}_2$ into equation (3.22) which yields

$$u_I(t) = -\sum_{i=1}^{n} \sqrt{\beta_i} \; z_i(t) \tag{3.23}$$

From equation (3.23) the gain of each integrator is seen to be the square root of each of the corresponding main diagonal elements in P. Furthermore, there is no coupling between integrators.

Three criteria are used to reflect the performance of the system and each is given attention in selecting the weighting parameters. First, the transient response is observed for desirable response characteristics. Secondly, the location of the closed loop roots determine the

degree of stability of the system. Ultimately, the RGC is considered when deemed necessary.

Therefore the following algorithm is suggested for the selection of the performance index weighting factors. First, the speed of reset is chosen by selecting β_1 because of its direct relation to the control. Then an appropriate value for α_1 is chosen to reduce ACE fluctuations and to set the quick speed response. Finally, γ_1 is adjusted to limit the RGC to an acceptable level.

CHAPTER 4

COMPOSITE SYSTEM ANALYSIS

Composite system analysis consists of determining the best control for the entire interconnected system. This procedure is not generally pursued in present day operation since each area is independent and is primarily concerned with supplying its own load. The problem of determining an optimal policy for each area with respect to the remainder of the interconnected system will be addressed in the next chapter.

The high order of the systems prohibits any meaningful analytical solution. Hopefully, the design concepts have been illustrated, and thus simulation studies of two and three area systems will demonstrate a numerical application of the concepts. In this study the following nominal numerical values are used for the control area:

$H_i = 5s$

$D_i = 8.33 \times 10^{-3}$ pu mw/hz

$T_{gi} = .08s$

$T_{Vi} = .3s$

$R_i = 2.4$ hz/pu mw

$\beta_{ai} = D_i + 1/R_i = .42458$ pu mw/hz

$P_{ri} = 2000$ mw

$T_{ij} = .545$ pu mw

$\Delta P_{Di} = .001$ pu mw

$F_0 = 60$ hz

$$T_i = .314 \text{ pu mw}$$

$$\frac{\partial P_{Di}}{\partial |E_i|} = 1.0 \text{ pu mw/pu v.}$$

4.1. Two-Area Interconnected System.

A study of a two-area interconnected system as in Figure 4 is undertaken to illustrate the development procedure of a controller algorithm. All aspects of the controller design will be considered including normal and abnormal operation, effect of different bias settings, unequal areas, QV control effect on PF operation, and the effect of different performance indices. These various topics will be developed from equations (3.19), (3.20) and (3.21).

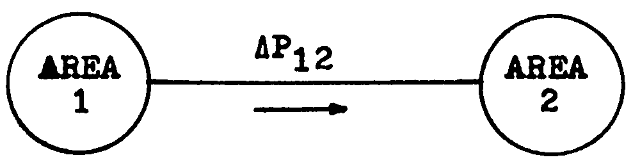

FIGURE 4. Simplified Two-Area System

A two-area system requires nine state variables for an independent description. The frequency deviation, the incremental generated power, the incremental valve position, and the IACE of each area are chosen as state variables. Only one state variable is required to describe the net interchange power deviation since there is only one tie line power flow between the areas. Clearly,

$$\Delta P_{tie_1} = \Delta P_{12}$$

$$\Delta P_{tie_2} = -a_{12}\Delta P_{12} = -\frac{P_{r1}}{P_{r2}}\Delta P_{12}$$

where a_{12} accounts for difference in the rated power of each area.

Therefore the following equations are applicable to a two-area system:

$$\dot{\hat{x}} = \hat{A}\hat{x} + \hat{B}u + \hat{D}v$$
$$\hat{J} = \frac{1}{2}\int_0^\infty (\hat{x}^T\hat{Q}\hat{x} + u^T Ru)dt. \tag{4.1}$$

where

$$\hat{x}^T = [\Delta F_1 \quad \Delta P_{g1} \quad \Delta P_{V1} \quad \Delta F_2 \quad \Delta P_{g2} \quad \Delta P_{V2} \quad \Delta P_{12} \quad IACE_1 \quad IACE_2].$$

$$\begin{bmatrix} u_1 \\ u_2 \end{bmatrix} = \begin{bmatrix} \Delta P_{c1} \\ \Delta P_{c2} \end{bmatrix} \qquad \begin{bmatrix} v_1 \\ v_2 \end{bmatrix} = \begin{bmatrix} \Delta P_{D1} \\ \Delta P_{D2} \end{bmatrix}$$

$$\hat{A} = \begin{bmatrix}
-\frac{D_1}{M_1} & \frac{1}{M_1} & 0 & 0 & 0 & 0 & -\frac{1}{M_1} & 0 & 0 \\
0 & -\frac{1}{T_{g1}} & \frac{1}{T_{g1}} & 0 & 0 & 0 & 0 & 0 & 0 \\
-\frac{1}{T_{V1}R_1} & 0 & -\frac{1}{T_{V1}} & 0 & 0 & 0 & 0 & 0 & 0 \\
0 & 0 & 0 & -\frac{D_2}{M_2} & \frac{1}{M_2} & 0 & \frac{1}{M_2}a_{12} & 0 & 0 \\
0 & 0 & 0 & 0 & -\frac{1}{T_{g2}} & \frac{1}{T_{g2}} & 0 & 0 & 0 \\
0 & 0 & 0 & -\frac{1}{T_{V2}R_2} & 0 & -\frac{1}{T_{V2}} & 0 & 0 & 0 \\
T_{12} & 0 & 0 & -T_{12} & 0 & 0 & 0 & 0 & 0 \\
B_1 & 0 & 0 & 0 & 0 & 0 & 1 & 0 & 0 \\
0 & 0 & 0 & B_2 & 0 & 0 & -a_{12} & 0 & 0
\end{bmatrix}$$

$$\hat{B}^T = \begin{bmatrix} 0 & 0 & \frac{1}{T_{V1}} & 0 & 0 & 0 & 0 & 0 & 0 \\ 0 & 0 & 0 & 0 & 0 & \frac{1}{T_{V2}} & 0 & 0 & 0 \end{bmatrix}$$

$$\hat{D}^T = \begin{bmatrix} -\frac{1}{M_1} & 0 & 0 & 0 & 0 & 0 & 0 & 0 & 0 \\ 0 & 0 & 0 & -\frac{1}{M_2} & 0 & 0 & 0 & 0 & 0 \end{bmatrix}$$

$$\hat{Q} = \begin{bmatrix} B_1^2 & 0 & 0 & 0 & 0 & 0 & \alpha_1 B_1 & 0 & 0 \\ 0 & \frac{\gamma_1}{T_{g1}^2} & -\frac{\gamma_1}{T_{g1}^2} & 0 & 0 & 0 & 0 & 0 & 0 \\ 0 & -\frac{\gamma_1}{T_{g1}^2} & \frac{\gamma_1}{T_{g1}^2} & 0 & 0 & 0 & 0 & 0 & 0 \\ 0 & 0 & 0 & B_2^2 & 0 & 0 & -\alpha_2 B_2 & 0 & 0 \\ 0 & 0 & 0 & 0 & \frac{\gamma_2}{T_{g2}^2} & -\frac{\gamma_2}{T_{g2}^2} & 0 & 0 & 0 \\ 0 & 0 & 0 & 0 & -\frac{\gamma_2}{T_{g2}^2} & \frac{\gamma_2}{T_{g2}^2} & 0 & 0 & 0 \\ \alpha_1 B_1 & 0 & 0 & -\alpha_2 B_2 & 0 & 0 & \alpha_1+\alpha_2 a_{12}^2 & 0 & 0 \\ 0 & 0 & 0 & 0 & 0 & 0 & 0 & \beta_1 & 0 \\ 0 & 0 & 0 & 0 & 0 & 0 & 0 & 0 & \beta_2 \end{bmatrix}$$

$$R = \begin{bmatrix} 1 & 0 \\ 0 & 1 \end{bmatrix}$$

The gain matrices for various performance indices are given in Appendix A.

4.1. Equal Area Simulation

In connection with the design of the controller algorithm, there is a need to establish the effect of certain parameters on system performance and to demonstrate the operation of the control scheme during normal and abnormal operation. As a matter of convenience, the study is divided into two groups: 1) variation of the performance index weightings, 2) variation of the bias setting for a fixed performance index weighting during normal and abnormal operation. The numerical values from the introduction to this chapter are used however, with $\Delta P_{D2} = 0$.

Performance Index Weightings

A collection of studies for various choices of α_1, β_1, and γ_1 of equation (3.21) are summarized in Table I. The measure of performance of each scheme is reflected by the transient response, the damping constant, and the maximum RGC.

The following observations are made using case C_0 as a reference (see Figures 5, 6, 7, and Table I):

1) C_3 and C_8 indicate that increasing the weight of Q relative to R improves the damping constant in exchange for an increase in the maximum RGC. The transient response is dominated by real roots. (See Figure 8 and Table I.)

2) The transient response is optimized [VAN], i.e., the closed loop roots are aligned such that all are fartherest away from the $j\omega$ axis simultaneously, when β_1 is greater than α_1 as evidenced by cases C_2 and C_4. (See Figures 5, 6, and 8.)

3) Speed of reset is determined by β_1. (See Figures 5 and 6.)

4) From cases C_7, C_8, and C_9, the increase of the γ_1 weighting significantly reduces the RGC at the expense of degrading the transient response and a reduction in damping constant. (See Figures 7 and 8 and Table I.)

TABLE I

Performance Index Weightings
Bias = β_{a1}

CASE	ACE α_1	IACE β_1	GRC γ_1	Maximum GRC %/min
C_0	1	1	0	11.40
C_1	10	1	0	15.00
C_2	1	10	0	15.35
C_3	10	10	0	17.40
C_4	.1	1	0	11.07
C_5	1	.1	0	9.72
C_6	.1	.1	0	9.06
C_7	1	1	.1	9.30
C_8	1	1	.5	6.40
C_9	1	1	1	5.09

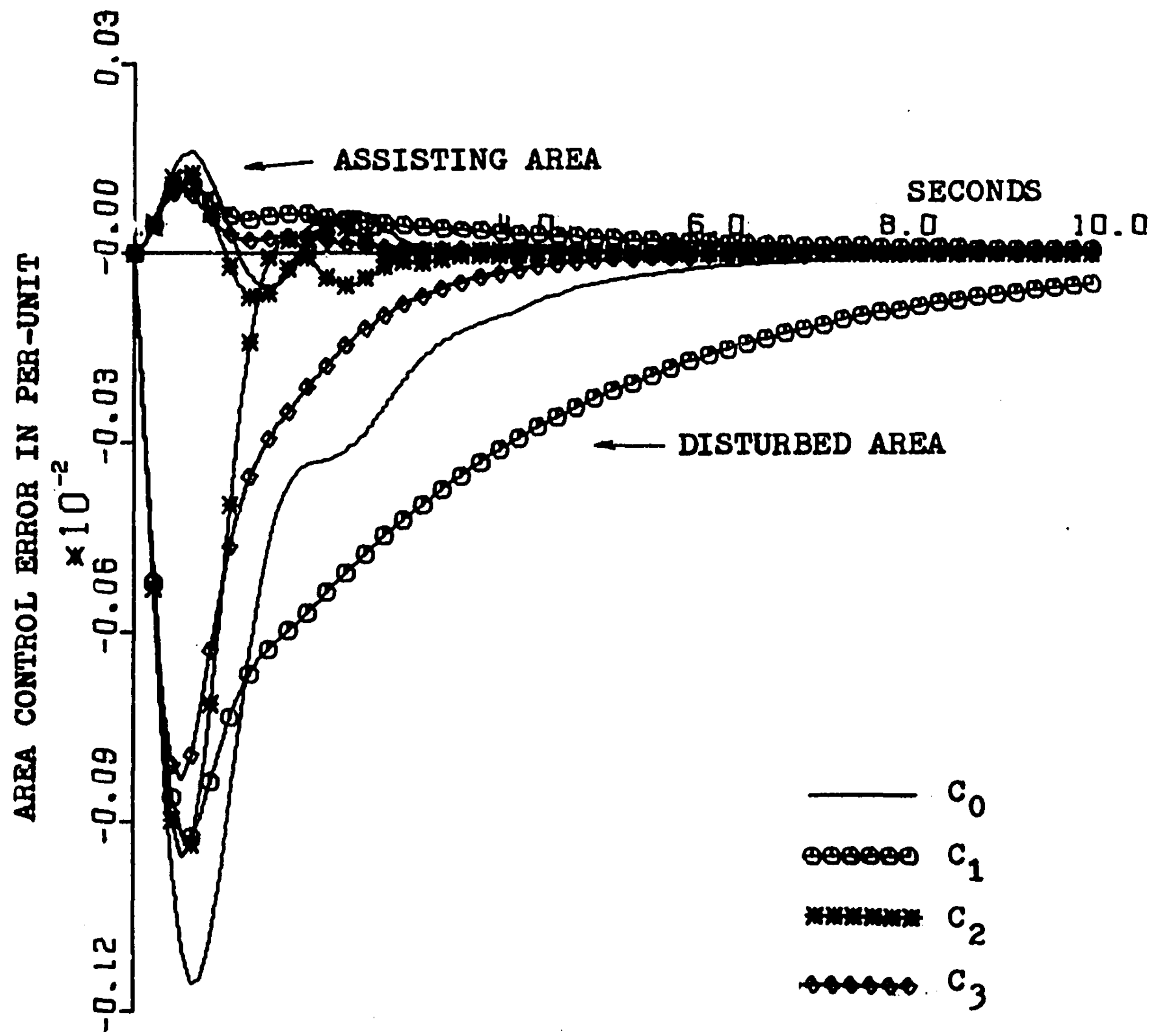

FIGURE 5. Performance Index Weighting ≥ 1

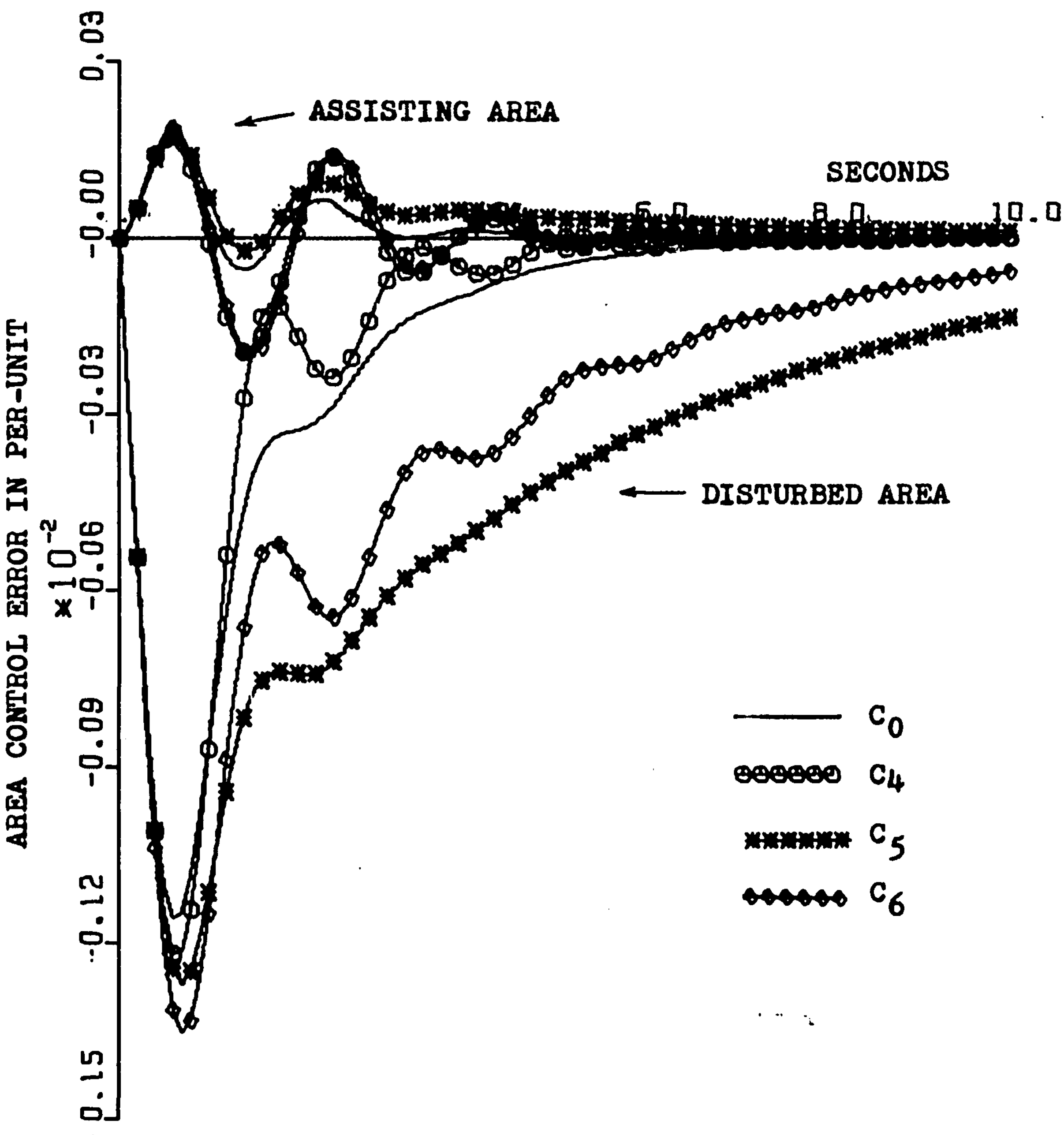

FIGURE 6. Performance Index Weighting ≤ 1

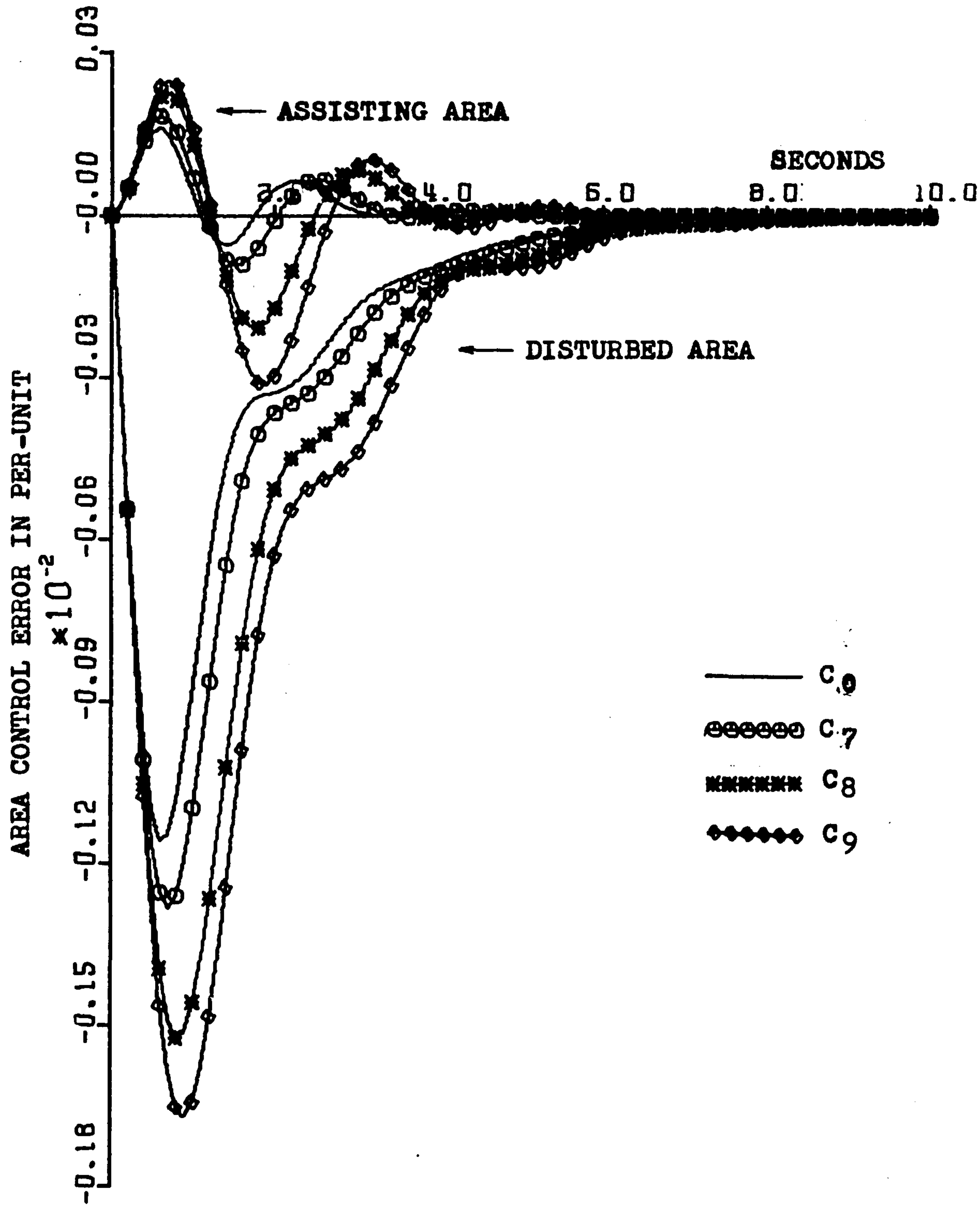

FIGURE 7. Performance Index with RGC Weighting

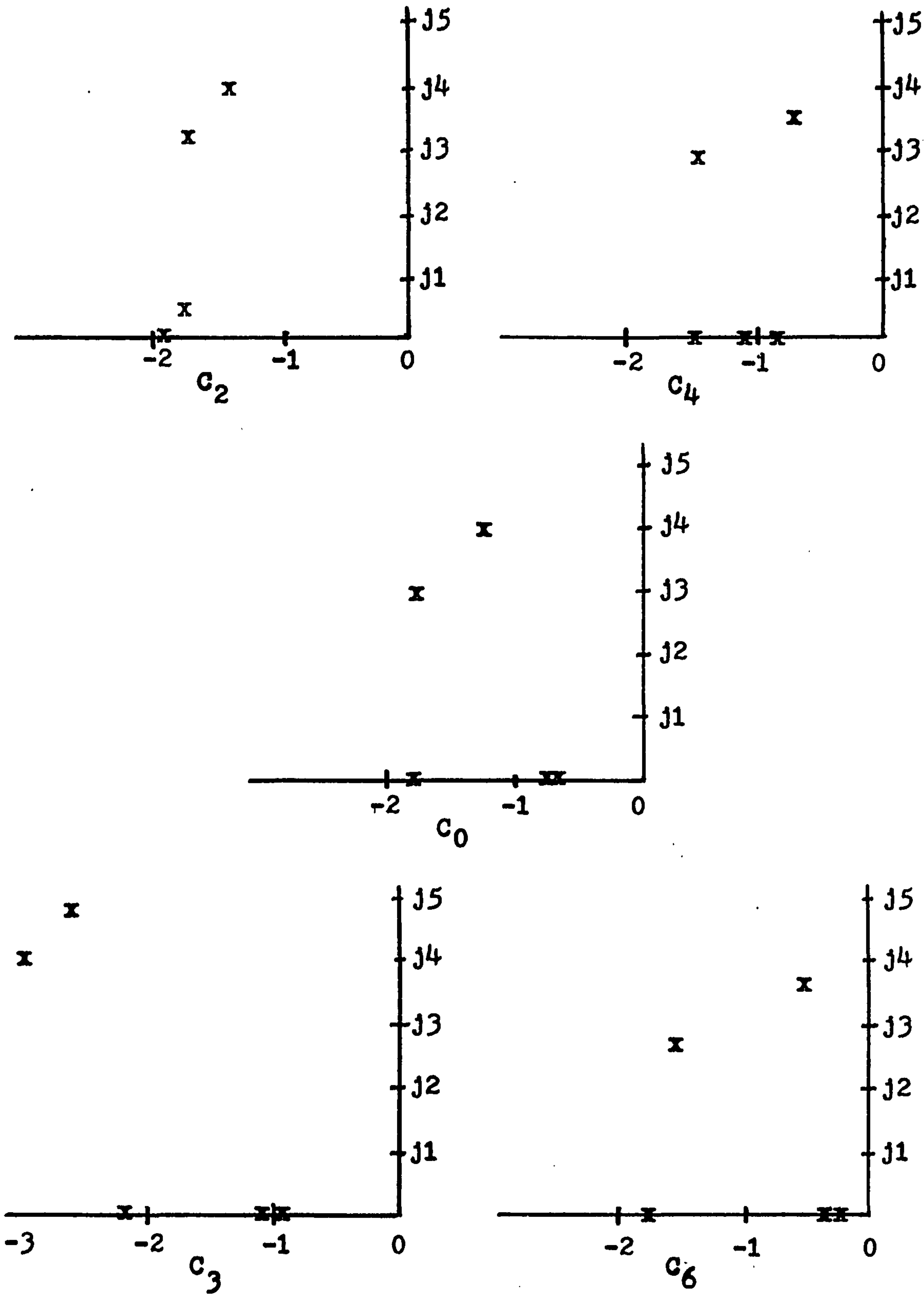

FIGURE 8. Closed Loop Roots for Various Performance Index Weightings

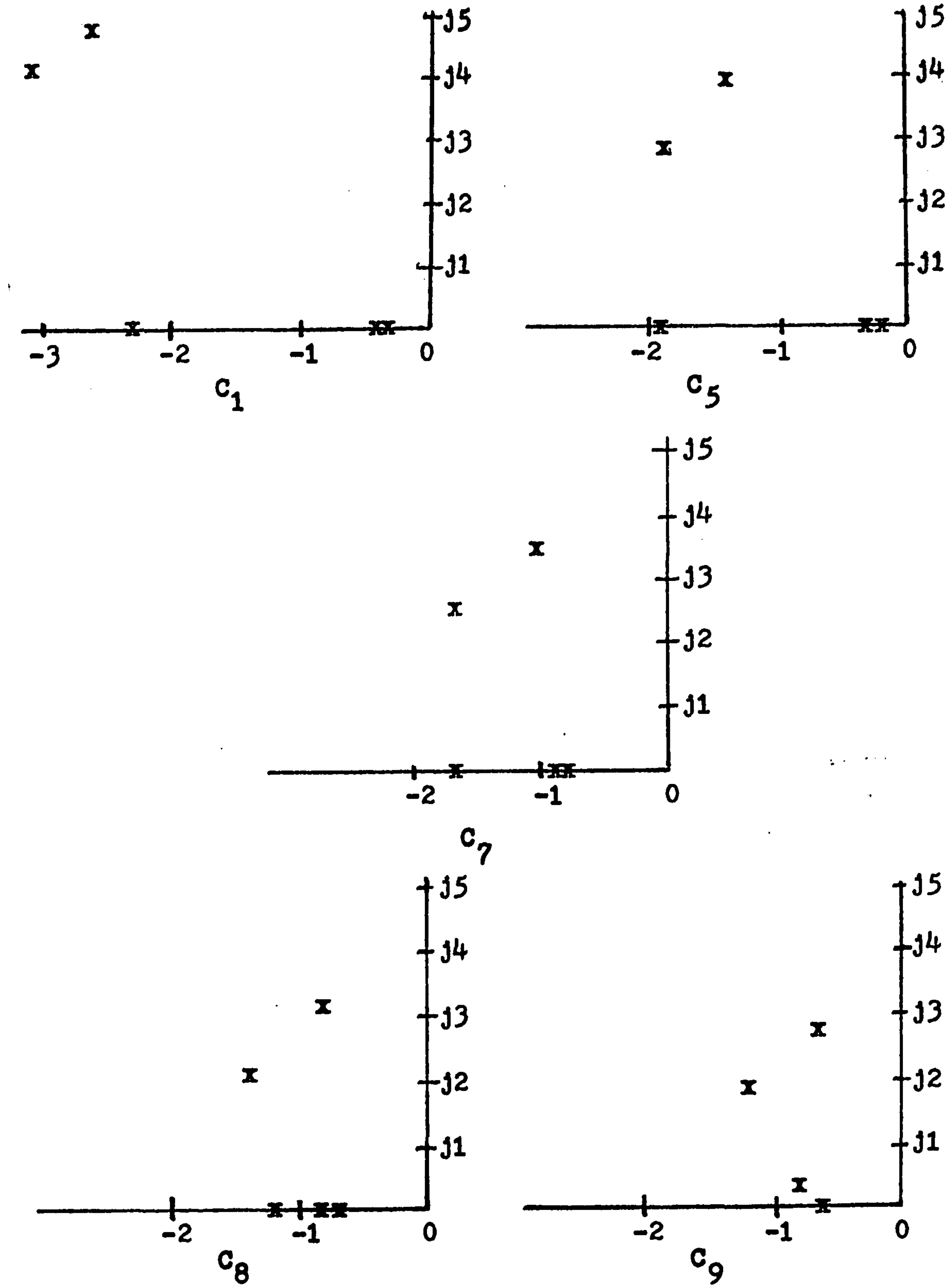

FIGURE 8. (Continued)

Bias Parameter Variation

The choice of the bias parameter determines the amount of offset between the frequency deviation and the net interchange power deviation. In several studies [CO1, EL2, KIR] the frequency bias constant is equated to the area frequency response characteristic (AFRC) β_{ai}. This value of bias insures that the static value of the ACE without supplementary control is zero following a step change in load. However, if supplementary control is used which contains the IACE, then the ACE will automatically return to zero regardless of the choice of bias following a step change in load during normal operation.

Additionally, the performance of the controller during abnormal mode of operation needs to be considered. Two particular properties, i.e., system stability and zero steady state ACE for the area giving aid following a step change in load, are demonstrated for various bias settings.

It has been suggested [EL2] that the bias choice for dynamic operation should not be based on static requirements. In that study [EL2] a bias value of one-half the AFRC is recommended for optimal performance of the system using a performance index which does not reflect the effect of the ACE. In a later discussion [CO2], it is stated that one-half the AFRC for the bias setting has been discarded because it does not work well in practice. Furthermore, the discussion [CO2] indicates that bias values greater than the AFRC work much better.

A study of the effect of various bias settings in Table II and Figures 9, 10, and 11 are based on a specific performance index, namely $\alpha_i = 1$, $\beta_i = 1$, and $\gamma_i = 0$. The following observations are made:

1) Larger bias settings cause a faster system response time

with more overshoot and a smaller ACE in the assisting area the area during normal operation. (See Figures 9 and 10.)

2) A bias setting equivalent to the AFRC has the largest damping constant during both normal and abnormal operation. When comparing small bias settings to large ones, the latter is seen to produce systems with a larger damping constant. (See Figure 11.)

3) Large RGC is associated with larger bias settings. (See Table II.)

4) Systems with large bias settings are dominated by complex roots while real roots dominate systems with small bias settings. (See Figure 11.)

These examples illustrate the variation in the performance that is associated with each bias setting. If different performance indices are used for each bias setting, then larger damping constant, improved transient response and lower RGC are possible. Finally, since the discussion [CO2] does not specify what is meant by the best performance, this study suffices to illustrate specific desirable properties associated with each bias setting.

TABLE II

Bias Variation

Bias	ACE α_i	IACE β_i	RGC γ_i	Maximum RGC %/Min
NORMAL OPERATION				
$\frac{1}{2}\beta_{ai}$	1	1	0	10.60
β_{ai}	1	1	0	11.40
$2\beta_{ai}$	1	1	0	13.30
ABNORMAL OPERATION				
$\frac{1}{2}\beta_{ai}$	1	1	0	6.08
β_{ai}	1	1	0	7.50
$2\beta_{ai}$	1	1	0	8.22

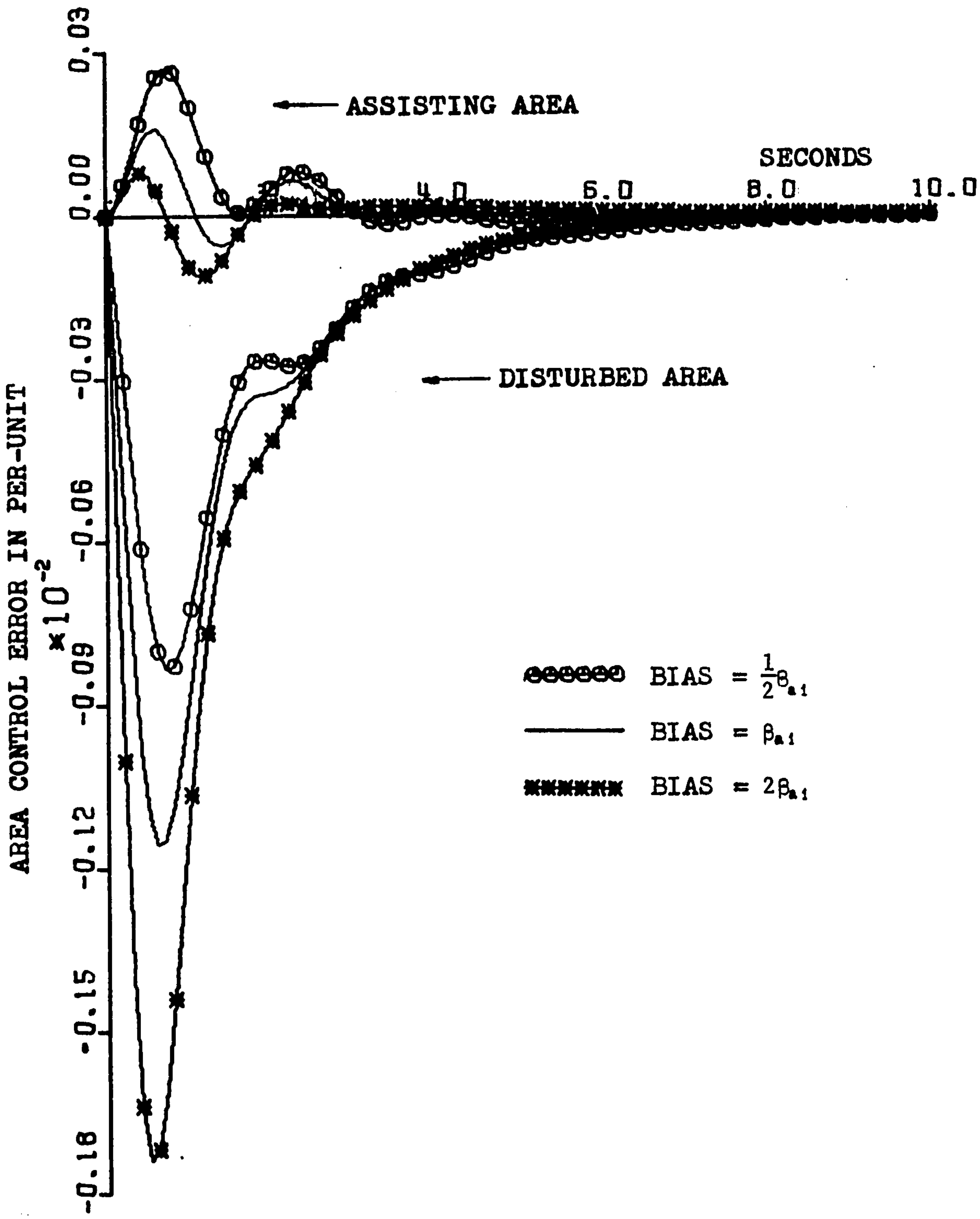

FIGURE 9. Bias Variation -- Normal Operation

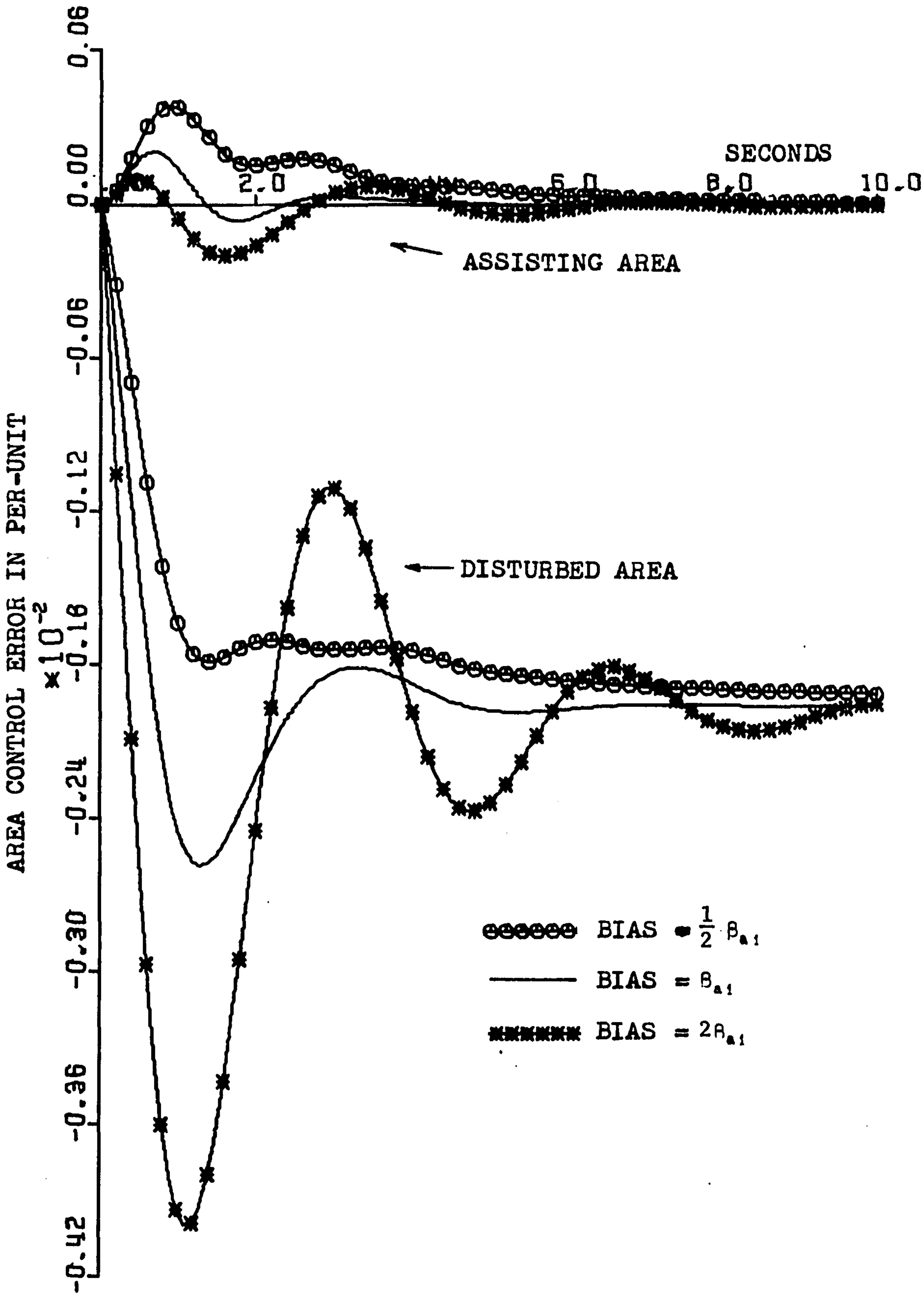

FIGURE 10. Bias Variation -- Abnormal Operation

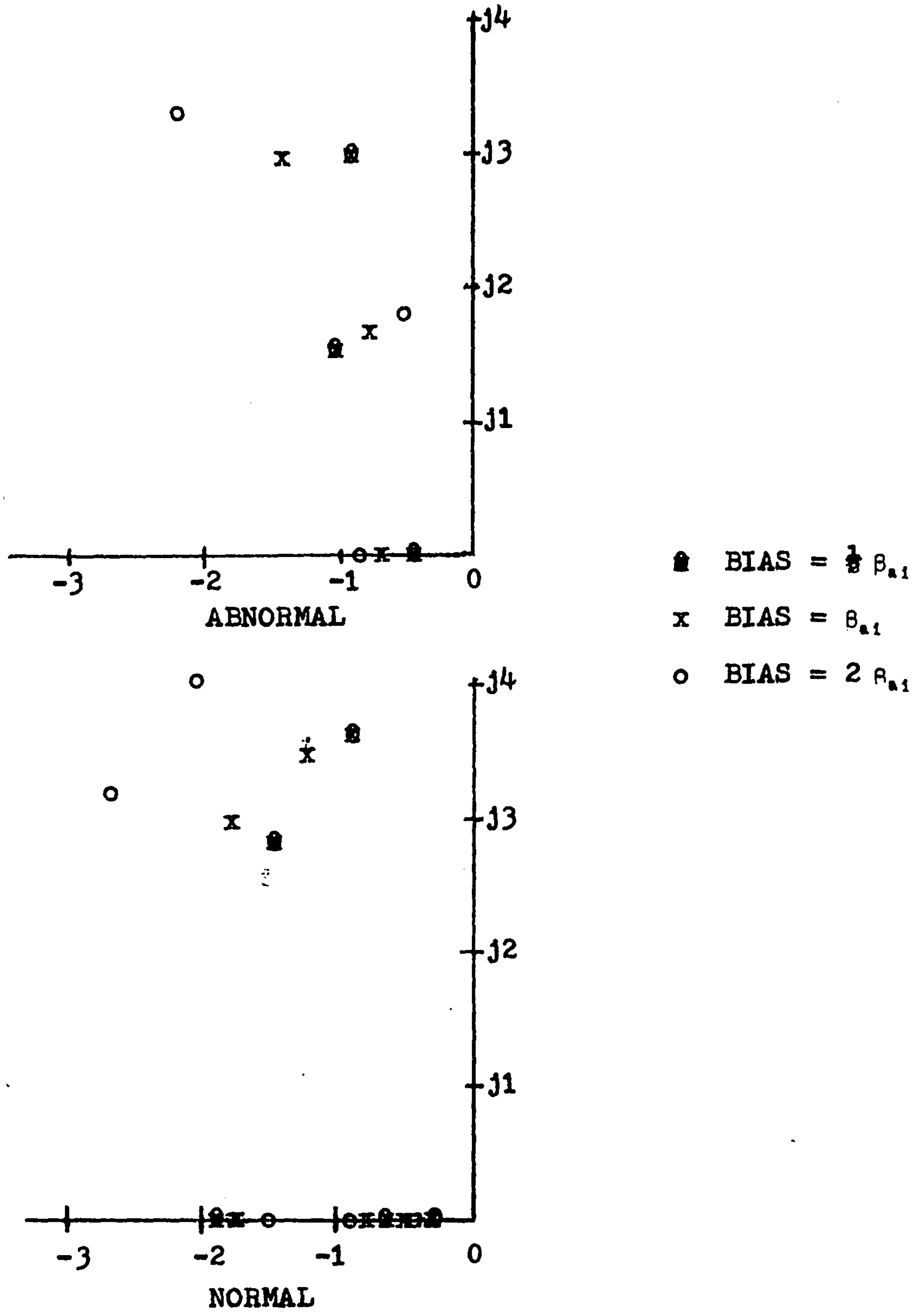

FIGURE 11. Closed Loop Roots for Various Bias Settings

4.2-2. Unequal Areas

This section is designed to demonstrate the effect of different area sizes upon the performance of an interconnected system. In each case a disturbance is introduced into the smaller area to measure the effect of the larger one on the former ones performance. Each interconnected system is comprised of two areas with one being an integral multiple of the other. The particular numerical examples are multiples of 2, 4, and 10 for the same performance index, namely $\alpha_1 = 1$, $\beta_1 = 1$, and $\gamma_1 = 0$. The results of the study are shown in Figures 12 and 13.

One of the most interesting properties of the optimal controller is that the ACE of the smaller area is virtually the same regardless of the size of the larger area. This result is obtained by a trade-off between the frequency and interchange power deviations. As the larger area increases in size, the frequency deviations in the smaller one swing positive as the power flow between the areas increases, thereby maintaining a near constant ACE. There is no significant change in the damping constant or in RGC.

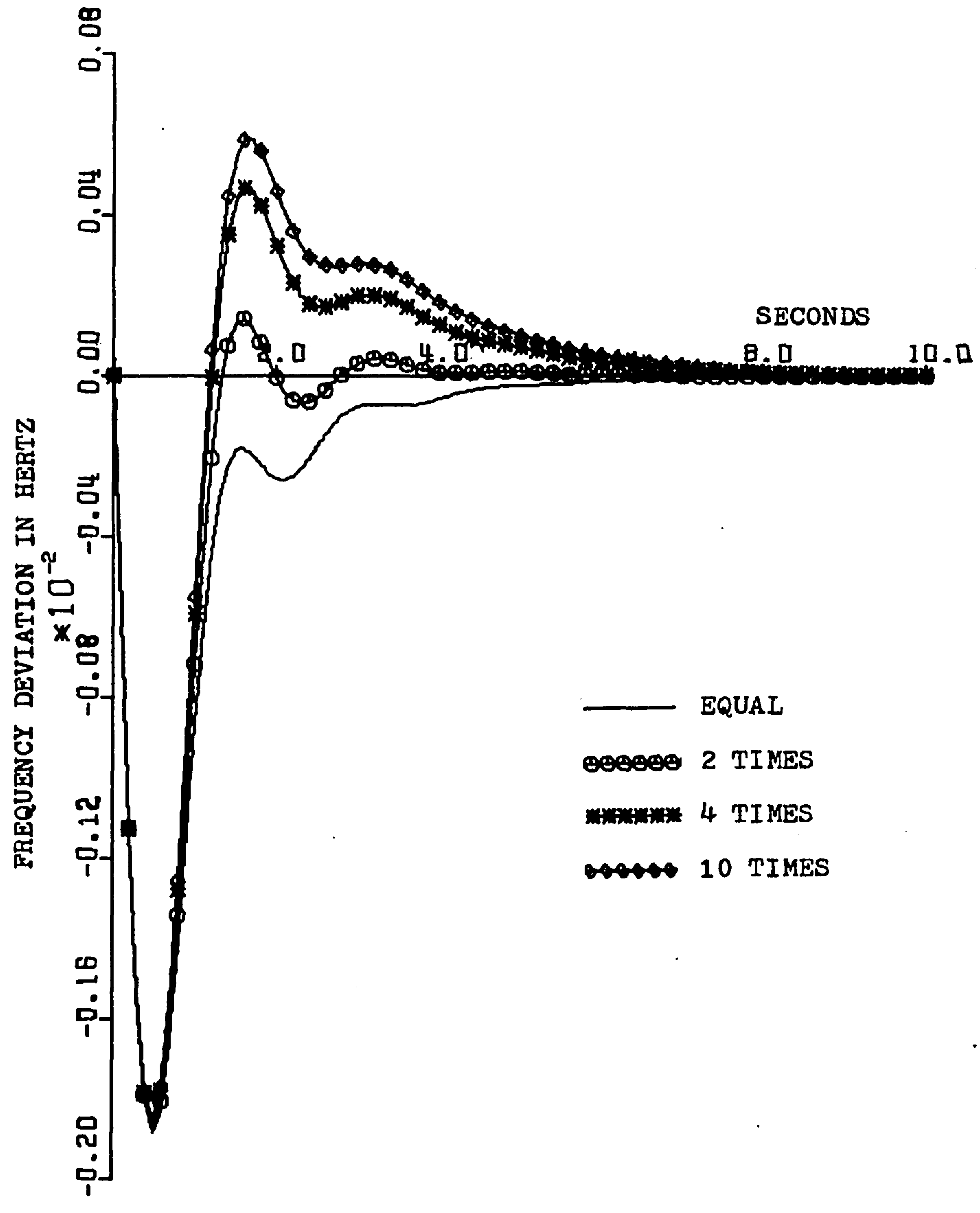

FIGURE 12. Frequency Deviation for the Smaller Area

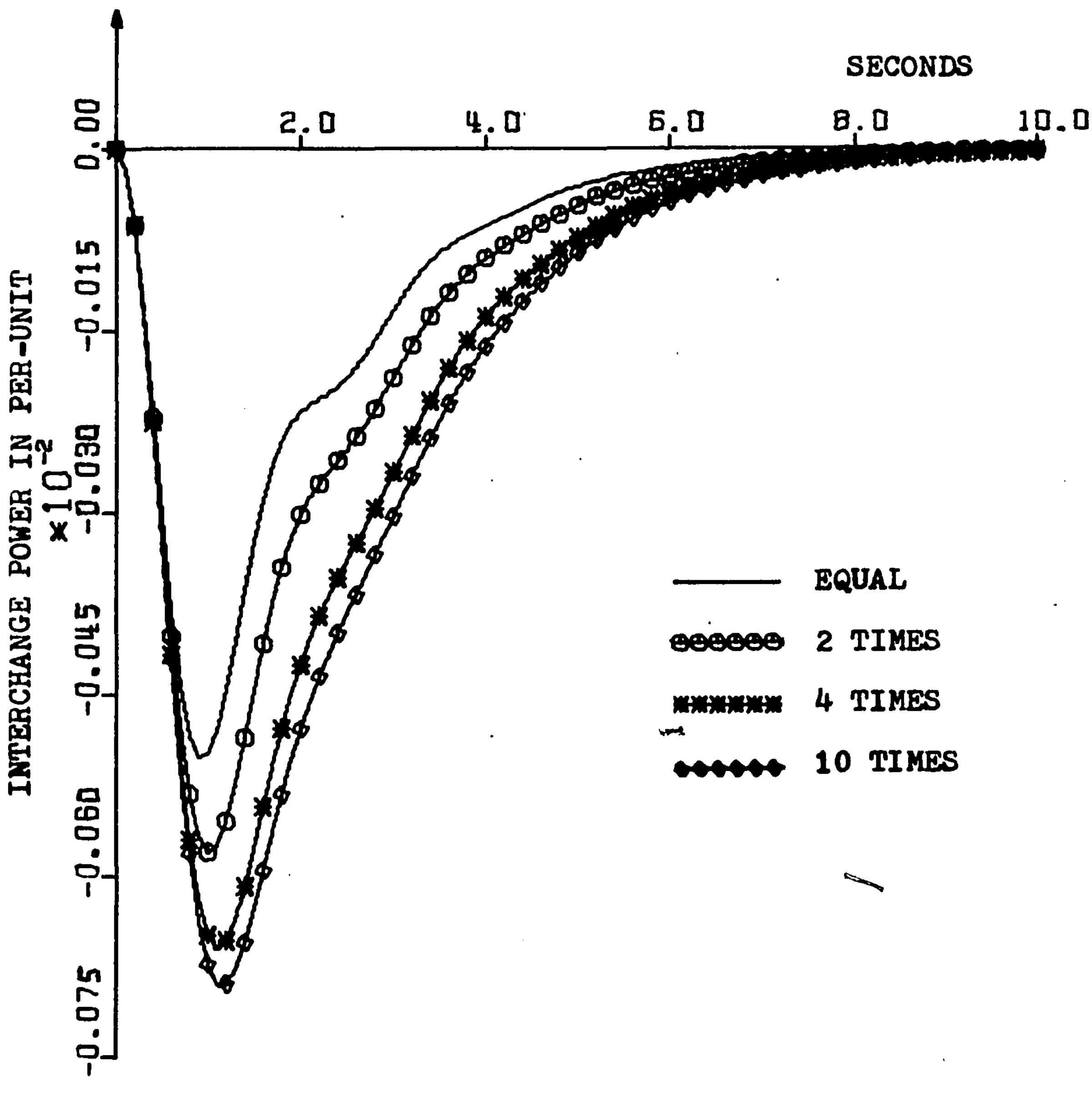

FIGURE 13. Interchange Power Deviation for Unequal Areas

4.1-3. QV Control Effect

In several studies [AND, DAV, KEL, YUY] optimal control theory has been applied to exciter control for transient stability. Other studies [DUR, EL3] have used optimal control theory for exciter control in an effort to influence the PF channel. The study in this section is directed toward this latter use of exciter control.

In section 3.2-2, the system equations have been modified to account for QV effects. This has been achieved by changing the $\hat{B}$-matrix to the form of equation (3.20) which for a two-area system is

$$\hat{B}^T = \begin{bmatrix} 0 & 0 & \frac{1}{T_{V1}} & 0 & 0 & 0 & 0 & 0 & 0 \\ 0 & 0 & 0 & 0 & 0 & \frac{1}{T_{V2}} & 0 & 0 & 0 \\ -\frac{1}{M_1}\left[\frac{\partial P_{D1}}{\partial |E_1|} + T_1\right] & 0 & 0 & \frac{1}{M_1}T_1 & 0 & 0 & 0 & 0 & 0 \\ -\frac{1}{M_2}T_2 & 0 & 0 & \frac{1}{M_2}\left[-\frac{\partial P_{D2}}{\partial |E_2|} + T_2\right] & 0 & 0 & 0 & 0 & 0 \end{bmatrix}.$$

It may be noted that the numerical values of T_1 and T_2 may be either positive or negative.

The R-matrix of the cost functional must be modified so that the two new controls are accommodated. The new matrix is

$$R = \begin{bmatrix} 1 & 0 & 0 & 0 \\ 0 & 1 & 0 & 0 \\ 0 & 0 & \omega_1 & 0 \\ 0 & 0 & 0 & \omega_2 \end{bmatrix}.$$

ω_1 and ω_2 are adjusted to penalize the effect of each QV control while the Q-matrix is held constant with $\alpha_i = 1$, $\beta_i = 1$, and $\gamma_i = 0$.

As stated in section 3.2-2, the sign of T_i must be given careful consideration. An examination of Figures 14 and 15 and Table III verifies this concern. The addition of QV control does significantly reduce the ACE magnitudes and reduces the RGC by effectively shedding load via changing the voltage. However the degree of effectiveness is determined by sign of T_i, hence the nominal state is important. The damping constant is virtually unaffected by QV control.

TABLE III

Effect of QV Control

ω_i	$\Delta P_{DE\,1}$	$\Delta P_{DE\,2}$	%		Maximum RGC %/Min
			$\Delta\|E_1\|$	$\Delta\|E_2\|$	
∞	.00100	0	0	0	11.40
POSITIVE T_i					
10	.00082	-.00003	-.0158	- 0057	10.38
1	.00067	-.00016	-.0665	-.0312	6.54
.1	.00060	-.00047	-.0797	-.0938	2.94
NEGATIVE T_i					
10	.00099	.00004	-.0026	.0077	11.22
1	.00086	.00018	-.0331	.0369	10.14
.1	-.00005	.00048	-.2092	.0956	6.24

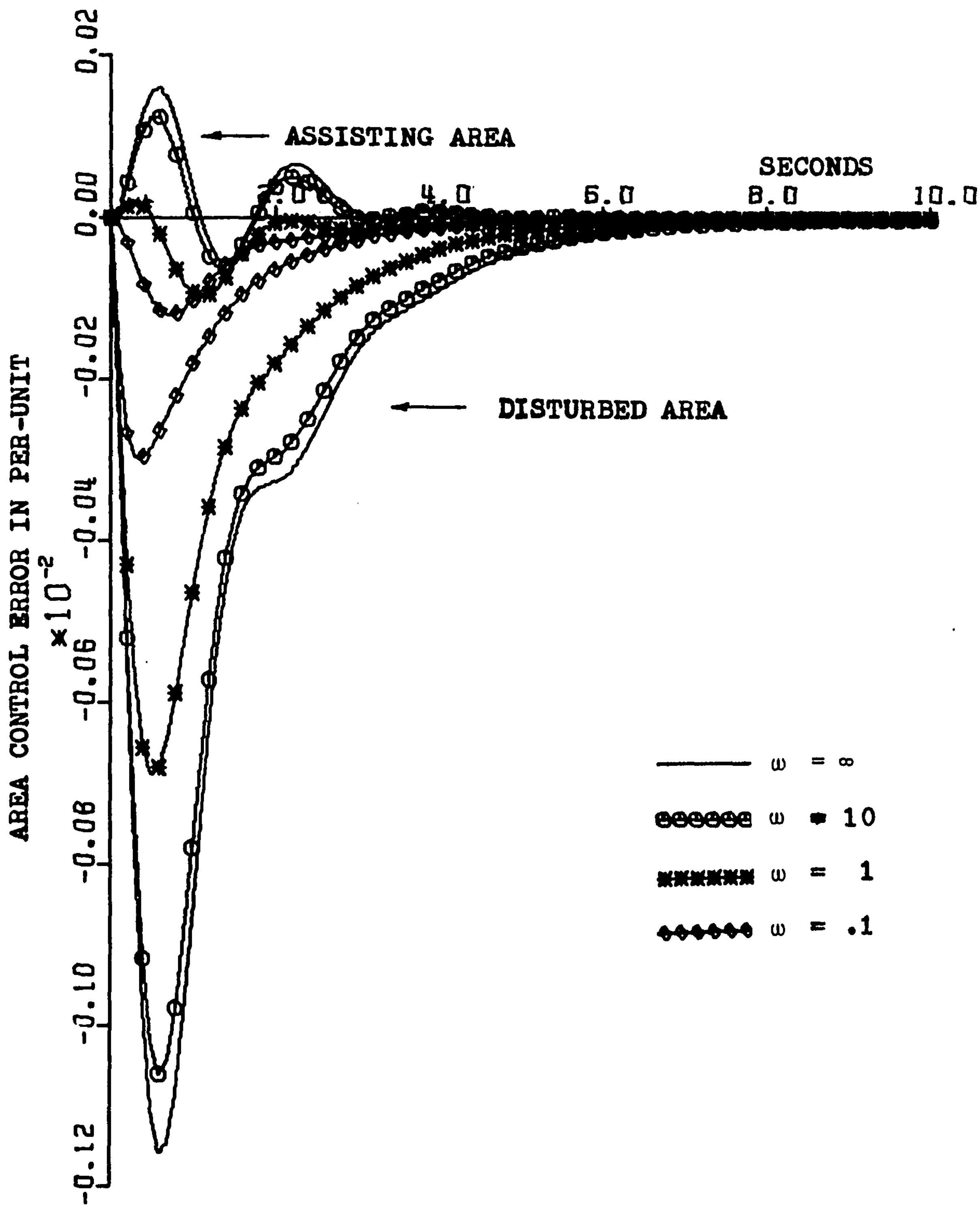

FIGURE 14. QV Effect for Positive T_1

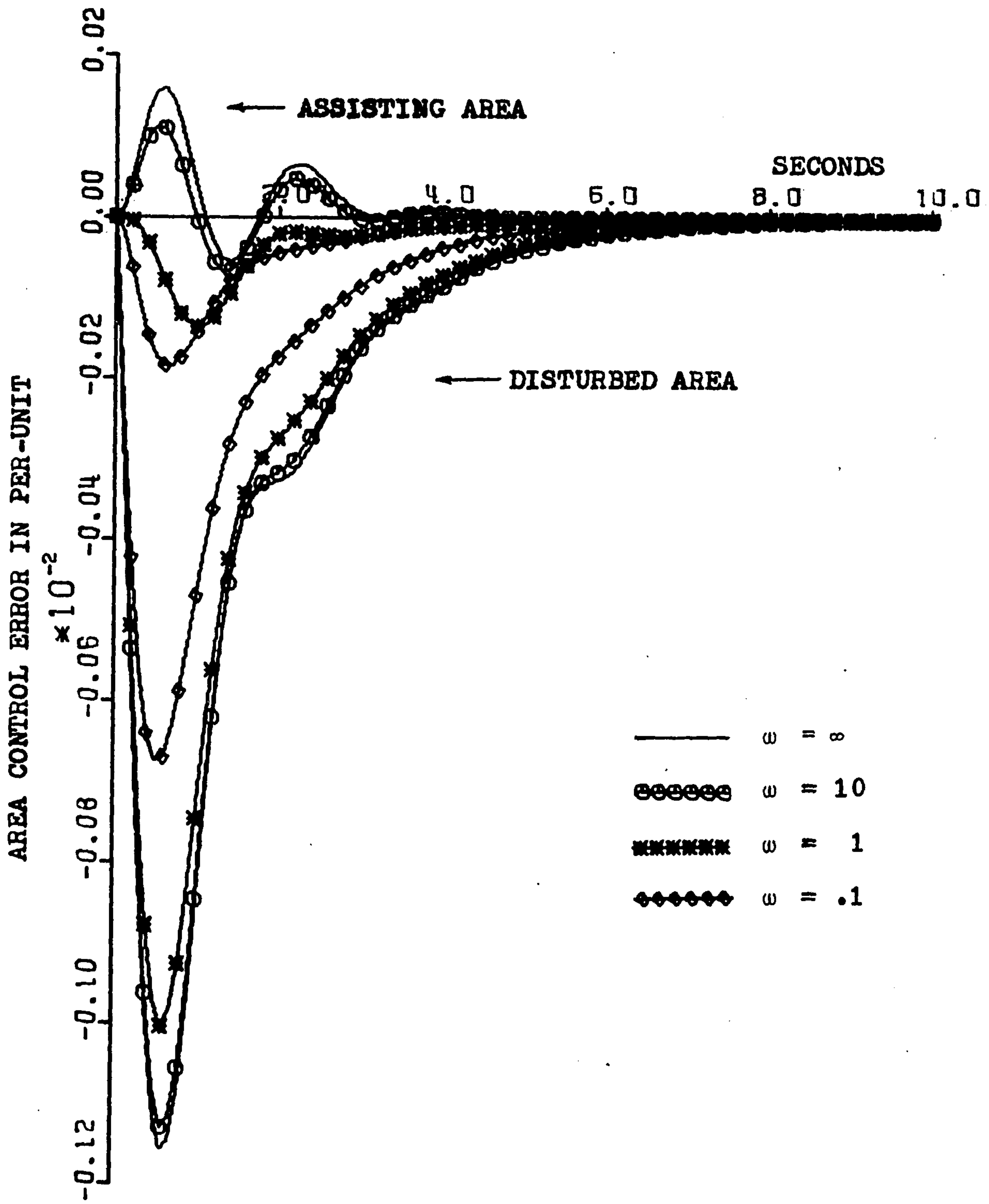

FIGURE 15. QV Effect for Negative T_1

4.2. Three Area System

A multi-area system has several inter-area tie lines thereby providing the opportunity for circulating power flows within the interconnected system. As power is exchanged among areas the direction of movement and the amount is determined by the size of the tie line and the dynamics of the areas. A two-area system does not exhibit the direction of movement property. The simplest multi-area system with these properties has three areas which is shown in Figure 16. The system equations for a three-area system are significantly different from those of a two-area system.

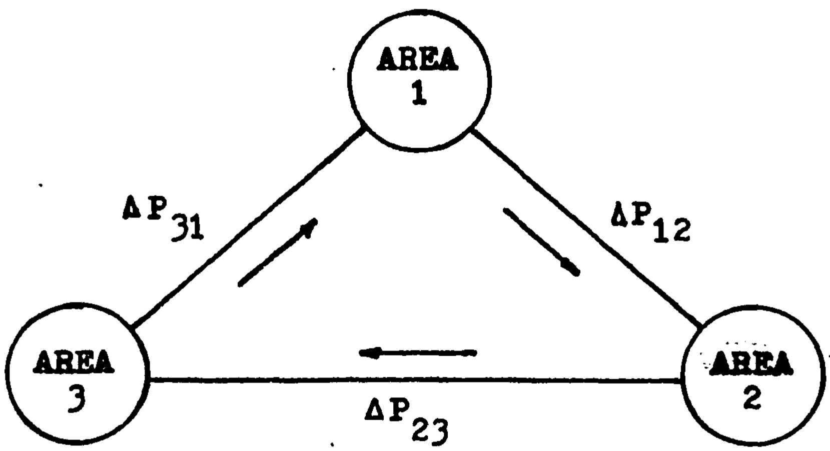

FIGURE 16. Simplified Three-Area System

In the case of a three-area system, there are at most three tie line power flows, but not all are independent. The following demonstrates the dependence of one of the tie line flows. The flows are

$$\Delta P_{12} = T_{12}(\delta_1 - \delta_2)$$

$$\Delta P_{23} = T_{23}(\delta_2 - \delta_3)$$

$$\Delta P_{31} = T_{31}(\delta_3 - \delta_1) \ .$$

The expression for ΔP_{31} does not introduce any information which is not present in the expressions for ΔP_{12} and ΔP_{23}. Therefore, by combining the expressions for ΔP_{12} and ΔP_{23}, it is easily shown that

$$\Delta P_{31} = -T_{31}\left[\frac{T_{23}\Delta P_{12} + T_{12}\Delta P_{23}}{T_{23}\ T_{12}}\right].$$

The expression for ΔP_{31} is simplified to

$$\Delta P_{31} = -\frac{T_{31}}{T_{12}}\Delta P_{12} - \frac{T_{31}}{T_{23}}\Delta P_{23}$$

or

$$\Delta P_{31} = -b_1\Delta P_{12} - b_2\Delta P_{23}\ .$$

Clearly, one power flow is dependent.

Therefore, the net interchange power for each area is

$$\Delta P_{tie_1} = \Delta P_{12} - \Delta P_{31} = (1+b_1)\Delta P_{12} + b_2\Delta P_{23}$$

$$\Delta P_{tie_2} = \Delta P_{23} - \Delta P_{12}$$

$$\Delta P_{tie_3} = \Delta P_{31} - \Delta P_{23} = -b_1\Delta P_{12} + -(b_2+1)\Delta P_{23}.$$

Now, the set of equations for an interconnected system with equal area dynamics but with different size tie line between areas can be expressed in the form of equation (4.1). The performance index is chosen as $\alpha_i = 1$, $\beta_i = 1$, and $\gamma_i = 0$. The matricies for $\hat{B}$, $\hat{D}$, and R and the vectors U and V are logically extended to accommodate the third area. The $\hat{A}$ and $\hat{Q}$ matrices are not as simple and thus they are given:

$$
\hat{A} = \begin{bmatrix}
-\frac{D}{M} & \frac{1}{M} & 0 & -\frac{(1+b_1)}{M} & 0 & 0 & 0 & -\frac{b_2}{M} & 0 & 0 & 0 & 0 & 0 & 0 \\
0 & -\frac{1}{T_g} & \frac{1}{T_g} & 0 & 0 & 0 & 0 & 0 & 0 & 0 & 0 & 0 & 0 & 0 \\
-\frac{1}{T_v R} & 0 & -\frac{1}{T_v} & 0 & 0 & 0 & 0 & 0 & 0 & 0 & 0 & 0 & 0 & 0 \\
T_{12} & 0 & 0 & 0 & -T_{12} & 0 & 0 & 0 & 0 & 0 & 0 & 0 & 0 & 0 \\
0 & 0 & 0 & \frac{1}{M} & -\frac{D}{M} & \frac{1}{M} & 0 & -\frac{1}{M} & 0 & 0 & 0 & 0 & 0 & 0 \\
0 & 0 & 0 & 0 & 0 & -\frac{1}{T_g} & \frac{1}{T_g} & 0 & 0 & 0 & 0 & 0 & 0 & 0 \\
0 & 0 & 0 & 0 & -\frac{1}{T_v R} & 0 & -\frac{1}{T_v} & 0 & 0 & 0 & 0 & 0 & 0 & 0 \\
0 & 0 & 0 & 0 & T_{23} & 0 & 0 & 0 & -T_{23} & 0 & 0 & 0 & 0 & 0 \\
0 & 0 & 0 & \frac{b_1}{M} & 0 & 0 & 0 & \frac{(b_2+1)}{M} & -\frac{D}{M} & \frac{1}{M} & 0 & 0 & 0 & 0 \\
0 & 0 & 0 & 0 & 0 & 0 & 0 & 0 & 0 & -\frac{1}{T_g} & \frac{1}{T_g} & 0 & 0 & 0 \\
0 & 0 & 0 & 0 & 0 & 0 & 0 & 0 & -\frac{1}{T_v R} & 0 & -\frac{1}{T_v} & 0 & 0 & 0 \\
B & 0 & 0 & 1+b_1 & 0 & 0 & 0 & b_2 & 0 & 0 & 0 & 0 & 0 & 0 \\
0 & 0 & 0 & -1 & B & 0 & 0 & 1 & 0 & 0 & 0 & 0 & 0 & 0 \\
0 & 0 & 0 & -b_1 & 0 & 0 & 0 & -(b_2+1) & B & 0 & 0 & 0 & 0 & 0
\end{bmatrix}
$$

$$\hat{Q} = \begin{bmatrix}
B^2 & 0 & 0 & B(1+b_1) & 0 & 0 & 0 & Bb_2 & 0 & 0 & 0 & 0 & 0 & 0 \\
0 & 0 & 0 & 0 & 0 & 0 & 0 & 0 & 0 & 0 & 0 & 0 & 0 & 0 \\
0 & 0 & 0 & 0 & 0 & 0 & 0 & 0 & 0 & 0 & 0 & 0 & 0 & 0 \\
B(1+b_1) & 0 & 0 & \left\{\begin{matrix}(1+b_1)^2 \\ +1 + b_1^2\end{matrix}\right\} & -B & 0 & 0 & \left\{\begin{matrix}b_2(1+b_1)-1 \\ +b_1(b_2+1)\end{matrix}\right\} & -b_1 B & 0 & 0 & 0 & 0 & 0 \\
0 & 0 & 0 & -B & B^2 & 0 & 0 & B & 0 & 0 & 0 & 0 & 0 & 0 \\
0 & 0 & 0 & 0 & 0 & 0 & 0 & 0 & 0 & 0 & 0 & 0 & 0 & 0 \\
0 & 0 & 0 & 0 & 0 & 0 & 0 & 0 & 0 & 0 & 0 & 0 & 0 & 0 \\
Bb_2 & 0 & 0 & \left\{\begin{matrix}b_2(1+b_1)-1 \\ +b_1(b_2+1)\end{matrix}\right\} & B & 0 & 0 & \left\{\begin{matrix}(b_2+1)^2 \\ +b_2^2 + 1\end{matrix}\right\} & -(b_2+1)B & 0 & 0 & 0 & 0 & 0 \\
0 & 0 & 0 & -b_1 B & 0 & 0 & 0 & -(b_2+1)B & B^2 & 0 & 0 & 0 & 0 & 0 \\
0 & 0 & 0 & 0 & 0 & 0 & 0 & 0 & 0 & 0 & 0 & 0 & 0 & 0 \\
0 & 0 & 0 & 0 & 0 & 0 & 0 & 0 & 0 & 0 & 0 & 0 & 0 & 0 \\
0 & 0 & 0 & 0 & 0 & 0 & 0 & 0 & 0 & 0 & 0 & 1 & 0 & 0 \\
0 & 0 & 0 & 0 & 0 & 0 & 0 & 0 & 0 & 0 & 0 & 0 & 1 & 0 \\
0 & 0 & 0 & 0 & 0 & 0 & 0 & 0 & 0 & 0 & 0 & 0 & 0 & 1
\end{bmatrix}$$

A collection of three-area systems with different sets of tie line sizes is displayed in Figure 17. In each case, an optimal controller is derived for the same performance index, namely $\alpha_i = 1$, $\beta_i = 1$, and $\gamma_i = 0$; then the system is simulated with a step disturbance in area 1 only. The significant results of these cases are summarized in Table IV. The numerical values in Table IV are recorded at the peak value of ACE_1 which occurs at about .6 second.

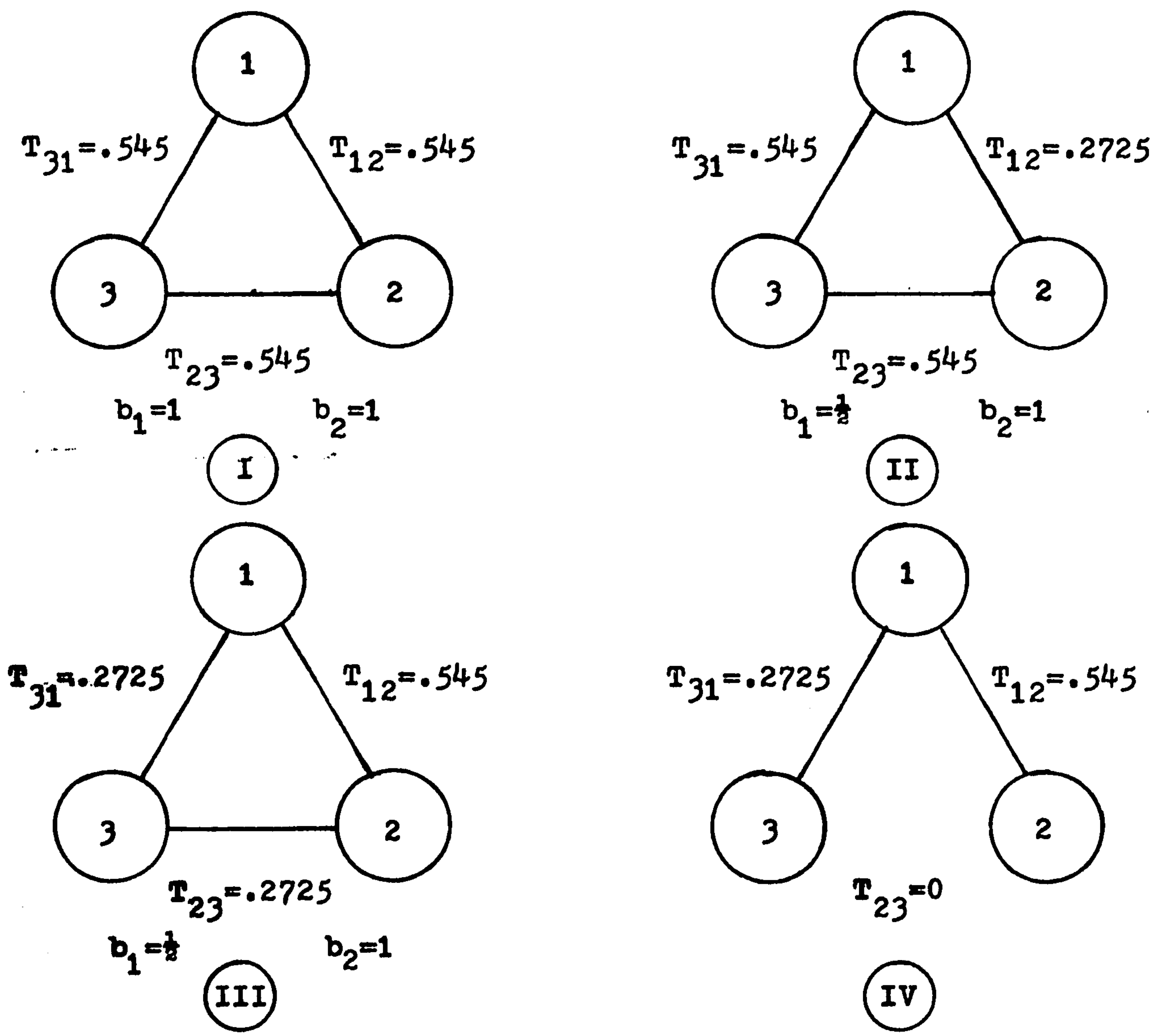

FIGURE 17. Three-Area Test Cases

TABLE IV

Three Area System

CASE	ACE 1	ACE 2	ACE 3	Net Interchange Power			Tieline Power Flow		
				P_1	P_2	P_3	ΔP_{12}	ΔP_{23}	ΔP_{31}
I	-.00128	.00014	.00014	-.00068	.00034	.00034	-.00034	0	.00034
II	-.00123	.00009	.00014	-.00055	.00021	.00034	-.00019	.00002	.00036
III	-.00123	.00014	.00009	-.00055	.00034	.00021	-.00036	-.00002	.00019
IV	-.00126	.00015	.00008	-.00056	.00037	.00019	-.00037	0	.00019

The following observations are made for the three-area studies:

1) For a system with equal tie lines, there is no power flow between the assisting areas, hence each area shares equally.

2) For a system with unequal tie lines, there is power flow between the assisting areas with the flow in the direction of the largest line.

3) The size of the tie line between the assisting areas had little effect on the system response.

4) If a two-area system is compared to a three-area system where the respective dynamics of each area and the tie lines are equal, it is noted that the latter system has smaller frequency deviations and a lower RGC than the former system. Although the effective transmission seen by the disturbed area of a three-area system is twice as large as that seen by the disturbed area of a two-area system, the net interchange power to the disturbed area is increased only by about 50 percent.

CHAPTER 5

DECOMPOSITION METHODS

In the previous chapter, the supplementary control for each area has been optimized for a performance index which reflects the operation of the entire interconnected system. This is not necessarily the most desirable form of control, and furthermore, this is not the approach employed in practice. Since each area is finally responsible for supplying its own load, an alternative control strategy is one that is optimal for its area only. In addition, an area does not want to take supplementary control action when the adjoining area has a disturbance.

In this chapter two different approaches are taken to derive an optimal controller for each area of the interconnected system. These local controllers are compared with the ones found by the method of Chapter 4. The methods of this chapter are examined for two reasons: 1) to derive an optimal controller for each area and 2) to introduce methods for optimizing a multi-area system via reduced computation effort.

5.1. Infinite Bus Analysis

One of the classical tools employed in power system studies has been the infinite bus characterization of systems. In stability analysis this type of approach has been used successfully. The exploitation of the infinite bus concept in effort to generate a local controller, i.e., one which employs information only about its own area, is of primary interest. For an interconnected system of several areas, an optimal control strategy requires a monumental computational effort and a good

communication channel for implementation. The infinite bus approach obviates these difficulties.

A system is classified as an infinite bus when a change in load power, either real or reactive, does not change the system frequency or voltage. In previous examples of this study the frequency of the adjoining areas does change. This is important because the frequency deviation determines the angle which is proportional to the power flow between the areas. For this study it is desirable to explore the possibility of treating adjoining areas as infinite buses for optimization purposes then simulate the system with full dynamics.

The infinite bus approach may be classified as a method of aggregation. If a dynamical system S_B is chosen to represent the significant dynamics of a system S_A, then S_B is said to be an aggregate model of S_A [WES]. The fundamental question arises as to what justification can be given for the selection of S_B. If a power system is "weakly coupled," i.e., the size of the tie lines are small, then there is little interaction between the areas. An infinite bus representation is justified. For large tie lines the system is classified as "stiffly coupled" and thus infinite bus representation may be invalid.

Using the infinite bus approach only requires modification to one control area equation, i.e., net interchange power. The infinite bus representation of the interchange power is

$$\Delta P_{tie_i} = \sum_{\substack{j=1 \\ j\neq i}}^{n} T_{ij}\delta_i . \tag{5.1}$$

With this representation each area is separated from the adjoining ones, and the effective tie line to the infinite bus area becomes the sum of the individual tie lines emanating from the area.

Using the infinite bus representation, the individual control areas become disjoint with one another. Therefore, the control for each area is derived from the variables of that area only. The optimization of an n-area system is converted to n optimizations of single areas. The system is reduced to independent 5th order sub-systems. The following procedure will consider a local controller using the full dynamics of the adjoining areas.

5.2. Suboptimal Control Analysis

Since it may be desirable to find a local controller for each area, a procedure which is dependent on the dynamics of the areas but independent of their control is explored. The class of deterministic controllers for the linear quadratic problem which does not incorporate all state variables of the system is called a suboptimal control. A method [LEV] for determining this suboptimal control has been presented and a numerical algorithm [BUC] for the application of the method is available.

The suboptimal control problem may be summarized as solving the equations

$$\begin{aligned} \dot{x}(t) &= Ax(t) + Bu(t) \\ g(t) &= Gx(t) \end{aligned} \tag{5.2}$$

for a control

$$u(t) = -Lg(t) = -LGx(t)$$

which minimizes the performance index

$$J = \frac{1}{2}\int_{0}^{\infty} [x^T(t)Qx(t) + u^T(t)Ru(t)]dt.$$

If the equations are written in closed loop form

$$\dot{x}(t) = (A-BLG)x(t),$$

then the solution to the problem is obtaining L. It has been shown [LEV] that L can be found independent of the initial conditions on equation (5.2) if the optimization process minimizes the expected value of J while assuming a uniformly distributed set of initial conditions on a unit hypersphere.

Before the suboptimal control concept can be applied, some modification to the power system equations is necessary. Only one control of the interconnected system is considered, therefore the B-matrix is reduced to one column. Furthermore, the IACE of the adjoining area is eliminated since it is not actually a part of the system dynamics. The cost functional reflects only one control area. The equations for a two-area and a three-area systems are reduced to 8th and 12th order respectively.

5.3. Simulation Results

An application of infinite bus (IB) and suboptimal control (SC) approaches to optimization is presented for both symmetrical two-area and symmetrical three-area systems. The numerical values from Chapter 4 are used and a disturbance is introduced into one area only. In the three-area case only one of the assisting area transient responses is shown since the other one is identical. The transient responses and the closed loop roots for each method of optimization are displayed in Figures 18 thru 22.

First consideration is directed at the IB approach. In the two-area studies for small tie line constant, i.e., $T_{12} \leq .545$ corresponding to a maximum transfer of 10% of the rated power of the area, only a slight degradation of the transient performance and some loss in damping constant is noted. For a large tie line constant ($T_{12} = 2.725$ corresponding to a maximum transfer of 50% of the rated power of the area), there is significant change in the transient performance and the damping constant. The three-area system performance is only degraded slightly. This is significant because the effective tie line constant of each area is 1.09 corresponding to a maximum transfer of 20% of the rated power of the area. From this study a tie line with a maximum capacity of 20% or less, IB optimization can be used effectively, however, for a tie line with a capacity of 50% the system performance is degraded significantly.

The SC procedure is obviously very successful. The degradation of the transient performance is only slight in all cases studied, however there is some loss of damping constant but not as severe as the IB method. Evidently, the SC procedure produces a local controller which very nearly optimizes the entire interconnected system.

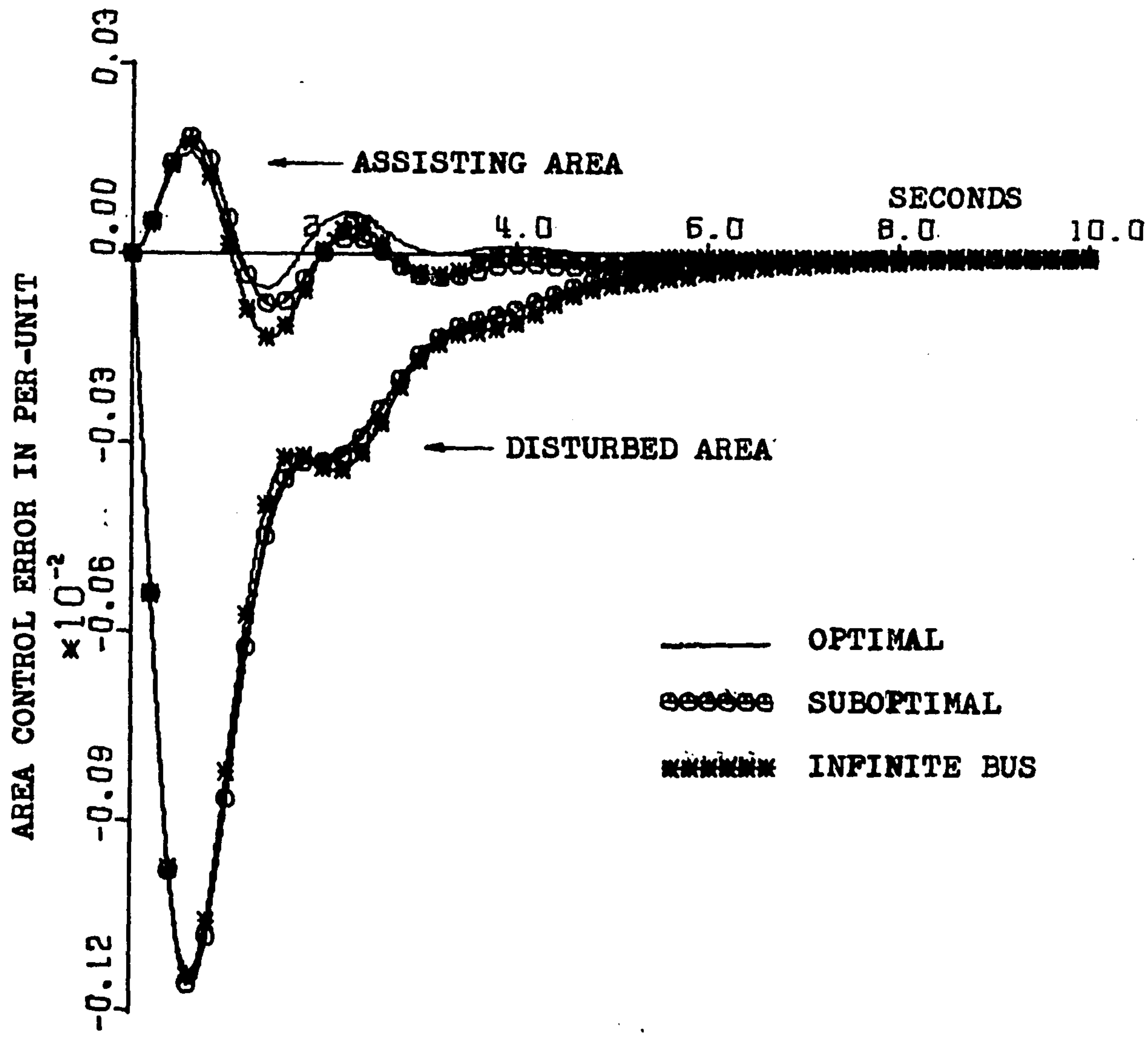

FIGURE 18. Two-Area System with T_{12} = .545

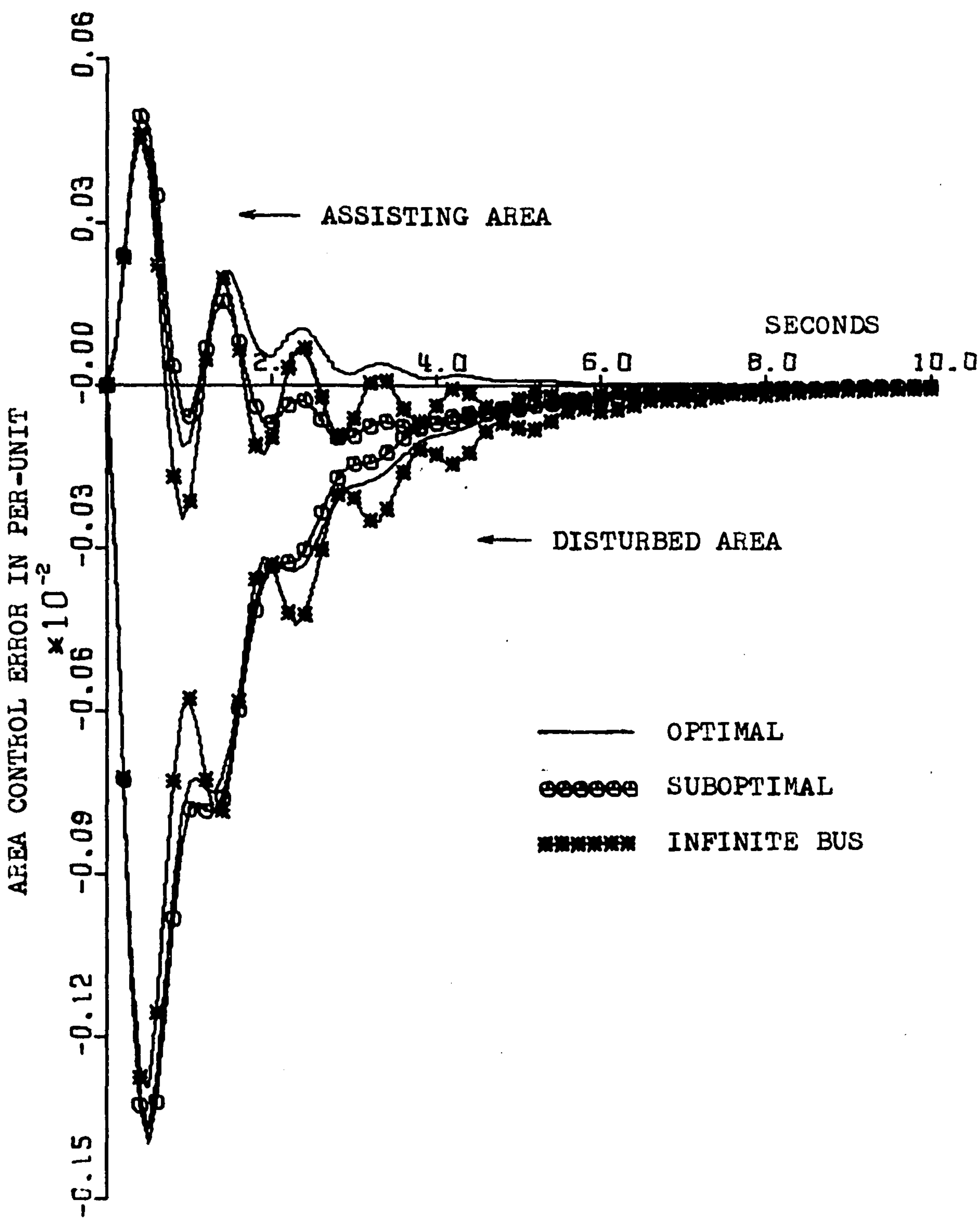

FIGURE 19. Two-Area System with T_{12} = 2.725

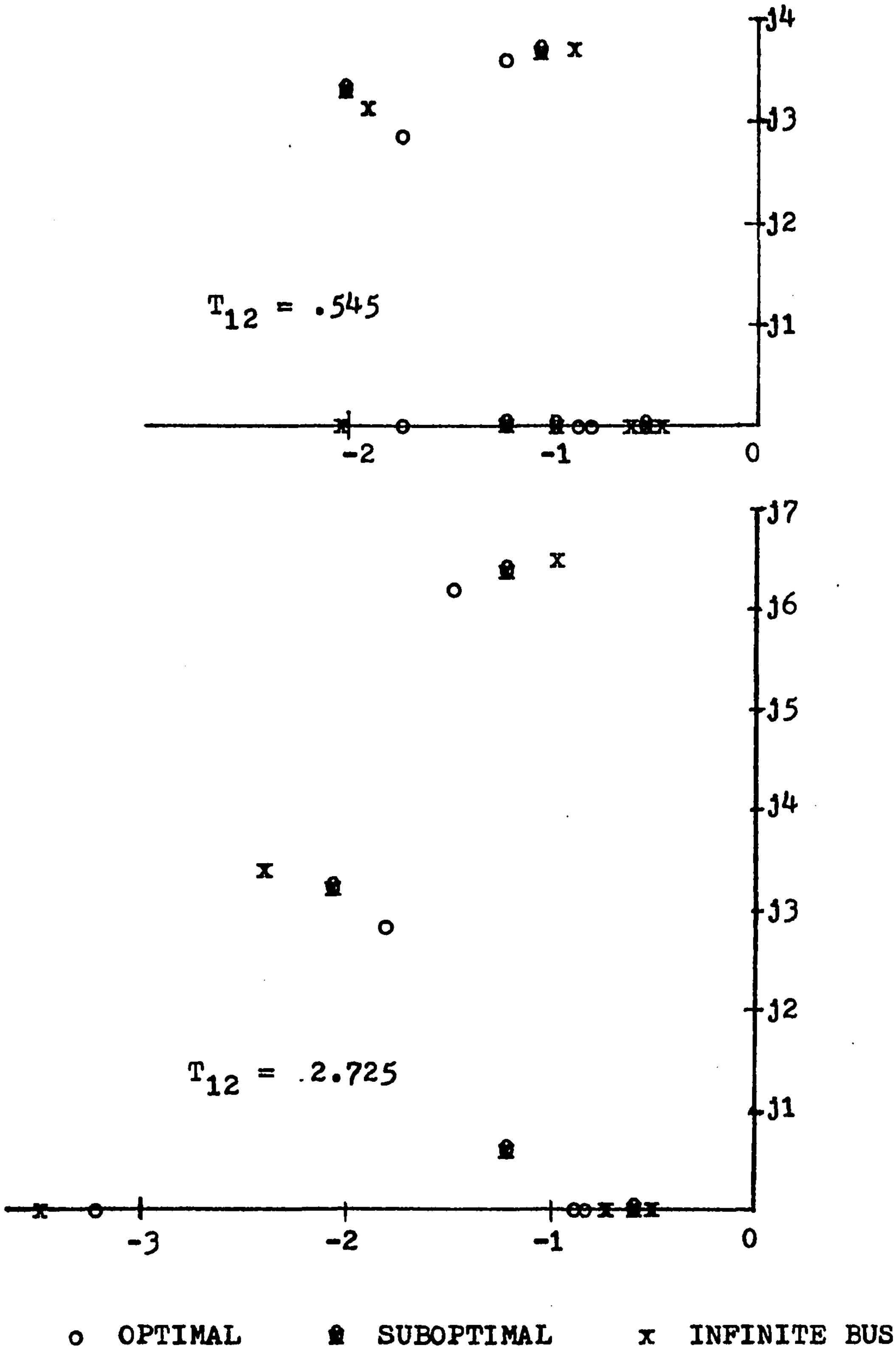

FIGURE 20. Closed Loop Roots for Two-Area Systems

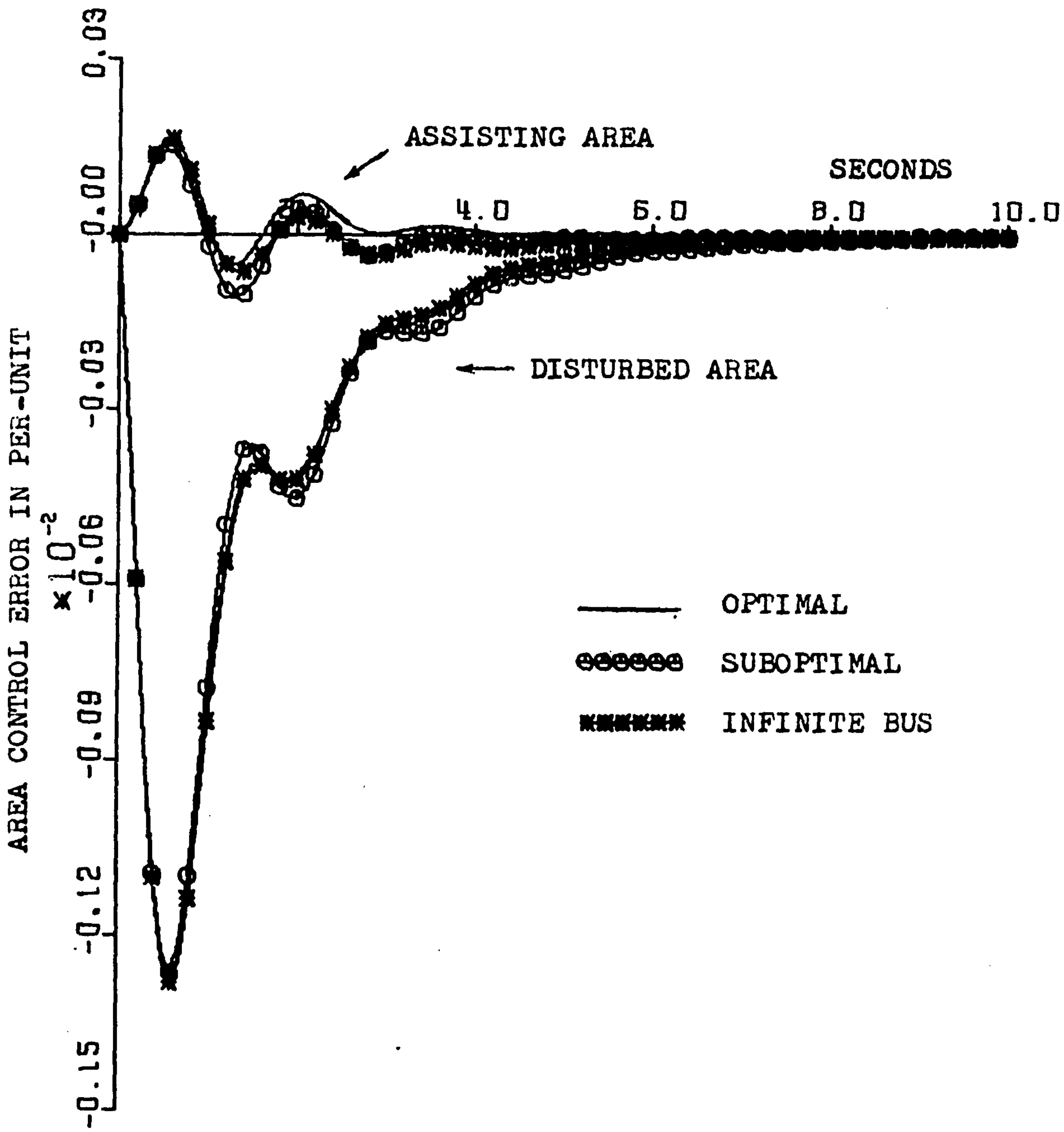

FIGURE 21. Three-Area System

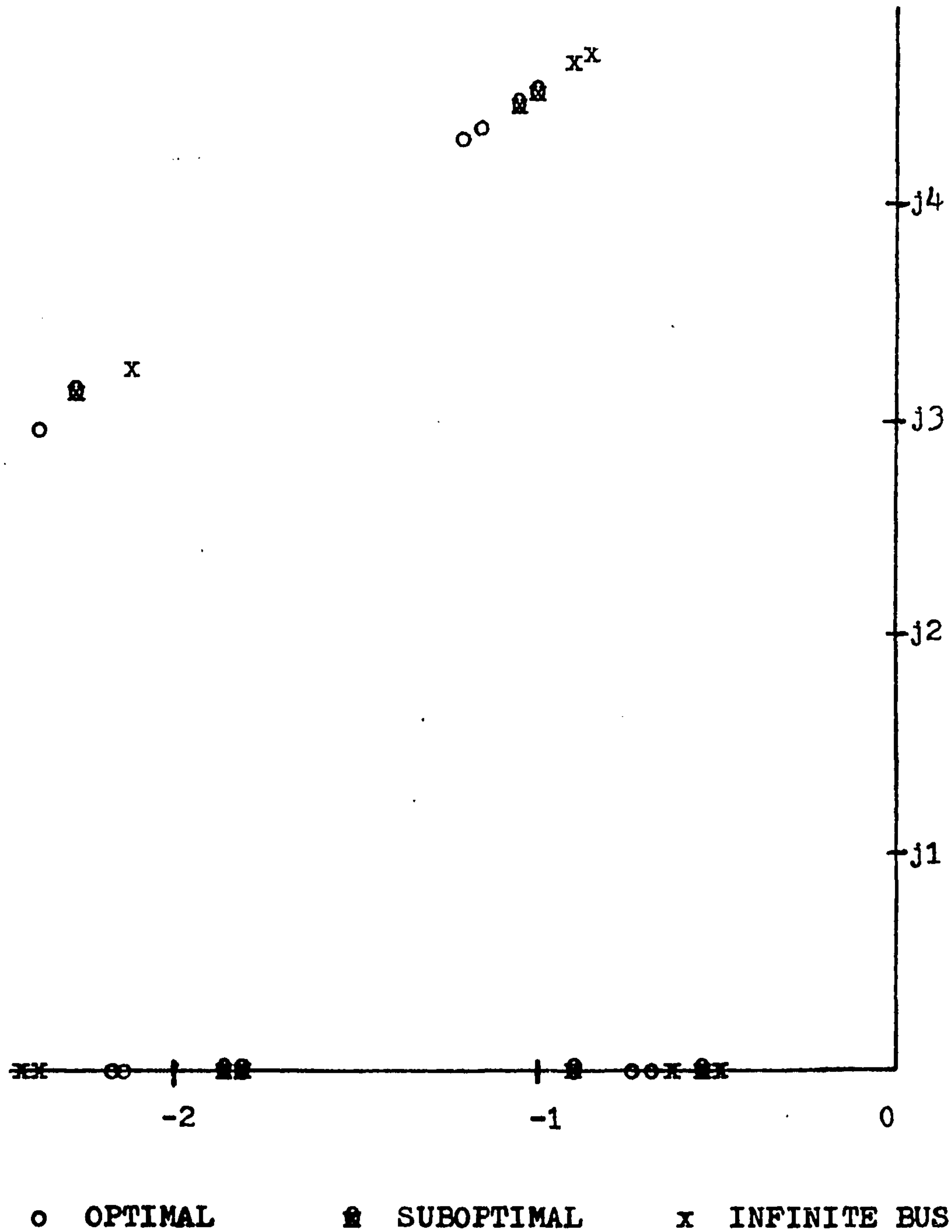

FIGURE 22. Closed Loop Roots for a Three-Area System

CHAPTER 6

CONCLUSIONS

This study has endeavored to clearly define the AGC problem and to demonstrate how optimal control theory can be applied and be compatible with present day practices and operating policies. A general procedure has been presented for the analysis of an n-area system with spceific application to two and three-area systems. The various control schemes are chosen to minimize a particular cost functional form. All cases have been tested for a step input disturbance.

Based on the cases used in this study the following conclusions have been formulated:

1) As the performance index is changed, i.e., α_1, β_1, and γ_1 are varied, a trade-off among transient response, damping constant, and the maximum RGC occurs.

2) The speed of reset is determined independent of the remainder of the optimization process for an optimal interconnected system controller.

3) A bias setting equal to the AFRC optimizes the transient response [VAN]. Systems which operate with a bias setting greater than the AFRC have a larger damping constant and faster responses than systems with bias settings less than the AFRC, but higher RGC.

4) For a system with two-areas of different size, there is an increase in frequency oscillation and an increase in power

flow between the areas but the ACE in the smaller area is unaffected for the cases considered in this study.

5) The use of QV control to influence the PF dynamics is successful in damping the ACE swings by shedding load and increasing the net interchange power via offsetting the voltage.

6) From the three-area study, a reduction in frequency deviation and maximum RGC are noted in exchange for an increase in net interchange power when compared to a similar two-area system.

7) The IB concept is successful in reducing computation effort and producing a good local controller.

8) A local controller produced by the SC approach is near optimal for the entire interconnected system.

REFERENCES

[AND] Anderson, J. H., "The Control of Synchronous Machines Using Optimal Control Theory," Proceedings of the IEEE, Vol. 59, No. 1, pps. 25-35, January 1971.

[ATH] Athans, Michael, "Special Issue on the Linear-Quadratic-Gaussian Problem," IEEE Transactions on Automatic Control, Vol. AC-16, No. 6, December 1971.

[BEN] Benson, A. R., W. F. Tinney, D. G. Wholgemuth, "Analysis of Dynamic Response of Electric Power System to Small Disturbances," Proceedings of the Power Industry Computer Applications Conference, pps. 247-259, 1965.

[BOH] Bohn, E. V., and S. M. Miniesy, "Optimum Load-Frequency Sampled-Data Control with Randomly Varying System Distrubances," IEEE Transactions on Power Apparatus and Systems, Vol. PAS-91, No. 5, pps. 1916-1924, September/October 1972.

[BUC] Buchert, Jr., G. J., P. M. Julich, and T. W. Reddoch, "A Numerical Algorithm for the Computation of Suboptimal Controls," Proceedings of the IEEE Decision and Control Conference, December 1972.

[CA1] Calovic, Milan, "Linear Regulator Design for a Load Frequency Control," IEEE Transactions on Power Apparatus and Systems, Vol. PAS-91, No. 6, pps. 2271-2285, November/December 1972.

[CA2] Calovic, Milan, "Power System Load and Frequency Control Using an Optimum Linear Regulator with Inegral Feedback," Paper No. 72, Fifth IFAC Congress, June 1972.

[CAV] Cavin, R. H., III, M. C. Budge, Jr., and P. Rasmussen, "An Optimal Linear Systems Approach to Load Frequency Control," IEEE Transactions on Power Apparatus and Systems, Vol. PAS-90, No. 6, pps. 2472-2482, November/December 1971.

[CO1] Cohn, Nathan, Control of Generation and Power Flow on Interconnected Systems, New York: John Wiley and Sons, Inc., 1966.

[CO2] Cohn, N., Discussion of "Optimum Megawatt-Frequency Control of Multi-area Electric Energy Systems," IEEE Transactions on Power Apparatus and Systems, Vol. PAS-89, No. 4, pps. 556-563, April, 1970.

[COL] Colombo, A., R. Federico, G. Guckstuhl, and A. Vian, "Determination of the Dynamic Response of Electrical Systems by Means of a Program," IEEE Transactions on Power Apparatus and Systems, Vol. PAS-87, No. 6, pps. 1411-1418, June 1968.

[CN1] Concordia, C. and L. K. Kirchmayer, "Tie Line Power and Frequency Control of Electric Power Systems," AIEE Transactions, Vol. 72, Part III, pps. 562-572, June 1953.

[CN2] Concordia, C. and L. K. Kirchmayer, "Tie Line Power and Frequency Control of Electric Power Systems--Part II," AIEE Transactions, Vol. 73, Part III-A, pps. 133-141, April 1954.

[CN3] Concordia C., S. B. Crary and E. E. Parker "Effect of Prime-Mover Speed Governor Characteristics on Power System Frequency Variations and Tie Line Power Swings," AIEE Transactions, Vol. 60, pps. 559-567, 1941.

[CRA] Crary, S. B., Power System Stability, New York: John Wiley and Sons, Inc. 1945.

[DAV] Davidson, E. J. and N. S. Rau, "The Optimal Output Feedback Control of a Synchronous Machine," IEEE Transactions on Power Apparatus and Systems, Vol. PAS-90, No. 5, pps. 2123-2134, September/October 1972.

[DUR] Durick, H. C., "Voltage Control to Damp Tie Line Power Oscillations," Lecture at 2nd Winter Institute on Electric Energy Engineering, December 1969.

[ELA] Elangovan, S. and A. Kuppurajulu, "Suboptimal Control of Power Systems Using Simplified Models," IEEE Transactions on Power Apparatus and Systems, Vol. PAS-90, No. 3, pps. 911-919, May/June 1972.

[EL1] Elgerd, O. I. and C. E. Fosha, "Load Frequency Control of Power Systems--A Reassessment in the Light of Modern Control Theory," Proceedings of the Southeastern Electric Exchange, 1969.

[EL2] Elgerd, O. I. and C. E. Fosha, "Optimum Megawatt-Frequency Control of Multi-area Electric Energy Systems," IEEE Transactions on Power Apparatus and Systems, Vol. PAS-89, No. 4, pps. 556-563, April, 1970.

[EL3] Elgerd, O. I. and C. E. Fosha, "The Megawatt-Frequency Control Problem: A New Approach Via Optimal Control Theory," IEEE Transactions of Power Apparatus and Systems, Vol. PAS-89, No. 4, pps. 563-576, April 1970.

[EL4] Elgerd, O. I., Electric Energy Systems Theory: An Introduction, New York: McGraw-Hill Book Company, 1971.

[HAM] Hamilton, H. B. and C. W. Eggers, Control and Operation of Electric Power Systems, Copyright, Univ. of Pittsburgh, 1970.

[HAN] Hanson, O. W., C. J. Goodwin, and P. L. Dandeno, "Influcence of Excitation and Spped Control Parameters in Stabilizing Intersystem Oscillations," IEEE Transactions on Power Apparatus and Systems, Vol. PAS-87, No. 5, pps. 1306-1313, May 1968.

[KA1] Kalman, R. E. and J. E. Bertram, "Control System Analysis and Design Via the 'Second Method' of Liapunov--I Continuous-Time Systems," Journal of Basic Engineering, pps. 371-393, June 1960.

[KA2] Kalman, R. E. "When Is a Linear Control System Optimal," Journal of Basic Engineering, pps. 51-60, March 1964.

[KEL] Kelley, D. H. and Ahm H. Rahim, "Closed Loop Optimal Excitation Control for Power System Stability," IEEE Transactions on Power Apparatus and Systems, Vol. PAS-90, No. 5, pps. 2135-2141, September/October 1971.

[KIR] Kirchmayer, Leon K., Economic Control of Interconnected Systems, New York: John Wiley and Sons, Inc., 1959.

[LEV] Levine, W. S. and M. Athans, "On the Determination of the Optimal Constant Output Feedback Gains for Linear Multivariable Systems," IEEE Transactions Automatic Control, Vol. AC-15, No. 1, pps 44-48, February 1970.

[LIA] Liacco, Thomas E., "The Adaptive Reliability Control System," IEEE Transactions on Power Apparatus and Systems, Vol. PAS-86, No. 5, pps. 517-531, May 1967.

[MEE] Meese, William, "A New Approach to R&D by the Electric Power Industry," Power Engineering Society Newsletter, pps. 7-11, September 1972.

[MES] Mesarovic, M. D., D. Macko, and Y. Takahara, Theory of Hierarchical, Multilevel Systems, New York: Academic Press, 1970.

[MI1] Miniesy, S. M. and E. V. Bohn, "Optimal Load Frequency Continuous Control with Unknown Deterministric Power Demand," IEEE Trans. on Power Apparatus and Systems, Vol. PAS-91, No. 5, pps. 1910-1915, September/October 1972.

[MI2] Miniesy, S. M. and E. V. Bohn, "Two-Level Control of Interconnected Power Plants," IEEE Transactions on Power Apparatus and Systems, Vol. PAS-90, No. 6, pps. 2749-2757, November/December 1971.

[NIC] Nicholson, Harold, "Hierarchical Control of a Multimachine Power System Model," IEEE Transactions on Power Apparatus and Systems, Vol. PAS-87, No. 7, pps. 1537-1548, July 1968.

[PO1] Porter, P., "Optimal Control of Multivariable Linear Systems Incorporating Integral Feedback," Electronics Letters, Vol. 7, No. 8, pps. 170-172, April 1971.

[PO2] Porter, B. and H. M. Power, "Controllability of Multivariable Systems Incorporating Integral Feedback, Electronics Letters, Vol. 6, No. 22, pps. 689-690, October 1970.

[PO3] Power, H. M. and B. Porter, "Necessary and Sufficient Conditions for Controllability of Multivariable Systems Incorporating Integral Feedback," Electronics Letters, Vol. 6, No. 25, pps 815-816, December 1970.

[QUA] Quazza, Giorgio, "Noninteracting Controls of Interconnected Electric Power Systems," IEEE Transactions on Power Apparatus and Systems, Vol. PAS-85, No. 7, pps. 727-741, July 1966.

[RE1] Reddoch, T. W., P. M. Julich, G. J. Buchert, Jr., O. T. Tan, and E. C. Tacker, "On the Use of Advanced Control in the Design of Automatic Generation Controllers," IEEE Winter Power Meeting Paper No. C 73 101-3, February 1973.

[RE2] Reddoch, T. W., P. M. Julich, O. T. Tan, and E. C. Tacker, "Models and Cost Functionals for Load Frequency Control in Interconnected Power Systems," Proceedings of the IEEE Decision and Control Conference, December 1971.

[RE3] Reddoch, T. W., P. M. Julich, O. T. Tan, and E. C. Tacker, "Optimization of the Load Frequency Controller Via Infinite Bus Analysis," Proceedings of Region III IEEE Conference, April 1972.

[RE4] Reddoch, T. W. and P. M. Julich, "A Discussion on the Application of Modern Optimal Control Theory to a Power System," THEMIS Technical Report No. 39 LSU-T-TR-39, September 1970.

[RO1] Ross, C. W., "Error Adaptive Control Computer for Interconnected Power Systems," IEEE Transactions on Power Apparatus and Systems, Vol. PAS-85, No. 7, pps. 742-749, July 1966.

[RO2] Ross, C. W. "A Comprehensive Direct Digital Load Frequency Controller," Proceedings of the Power Industry Computer Applications Conference, pps. 231-238, 1967.

[RO3] Ross, C. W., and Green, Thomas A., "Dynamic Performance Evaluation of a Computer Controlled Electric Power System," IEEE Transactions on Power Apparatus and Systems, Vol. PAS-91, No. 3, pps 1158-1165, May/June 1972.

[SC1] Schleif, F. R. and J. H. White, "Damping for the Northwest--South-West Tie Line Oscillations--An Analog Study," IEEE Transactions on Power Apparatus and Systems, Vol. PAS-85, No. 12, pps. 1239-1247, December 1966.

[SC2] Schleif, F. R., H. D. Hunkins, G. E. Martin, and E. E. Hattan, "Excitation Control to Improve Powerline Stability," IEEE Transactions on Power Apparatus and Systems, Vol. PAS-87, No. 6, pps. 1426-1434, June 1968.

[SC3] Schleif, F. R., H. D. Hunkins, E. E. Hattan and W. B. Gish, "Control of Rotating Exciters for Power System Damping: Pilot Applications and Experience," IEEE Transactions on Power Apparatus and Systems, Vol. PAS-88, No. 8, pps. 1259-1266, August 1969.

[VAN] Van Ness, J. E., "Root Loci of Load Frequency Control Systems," IEEE Transactions (Power Apparatus and Systems-supplement), pps. 712-726, 1963.

[WIS] Wismer, David A., Optimization Methods for Large-Scale Systems, New York: McGraw-Hill Co., 1971.

[YUY] Yu, Y. N., K. Vongsuriya, and L. N. Wedman, "IEEE Transactions on Power Apparatus and Systems, Vol. PAS-89, No. 1, pps. 55-62, January 1970.

APPENDIX A

The following matrices represent the optimal gain coefficients for the two-area cases analyzed in sections 4.1 and 5.3. The following notation is adopted for interfacing these matrices with the material presented in the text:

$$u = K_g \hat{x}$$

where K_g is an $m x(n+r)$ matrix and

$$\hat{x}^T = [\, F_1 \quad P_{g1} \quad P_{V1} \quad F_2 \quad P_{g2} \quad P_{V2} \quad P_{12} \quad IACE_1 \quad IACE_2] \ .$$

K_g for each case is as follows:

Case C_0 from Table I

$$\begin{bmatrix} -.424 & -.661 & -.163 & .079 & .115 & .026 & .176 & -1.000 & .000 \\ .079 & .115 & .026 & -.424 & -.661 & -.163 & -.176 & .000 & -1.000 \end{bmatrix}$$

Case C_1 from Table I

$$\begin{bmatrix} -1.386 & -1.719 & -.386 & .284 & .271 & .052 & -.191 & -.994 & .000 \\ .284 & .271 & .052 & -1.386 & -1.719 & -.386 & .191 & .000 & -.994 \end{bmatrix}$$

Case C_2 from Table I

$$\begin{bmatrix} -.863 & -1.135 & -.267 & .130 & .147 & .031 & -.034 & -3.162 & .000 \\ .130 & .147 & .031 & -.863 & -1.135 & -.267 & .034 & .000 & -3.162 \end{bmatrix}$$

Case C_3 from Table I

$$\begin{bmatrix} -1.712 & -1.978 & -.432 & .319 & .282 & .052 & -.522 & -3.162 & .000 \\ .319 & .282 & .052 & -1.712 & -1.978 & -.432 & .522 & .000 & -3.162 \end{bmatrix}$$

Case C_4 from Table I

$$\begin{bmatrix} -.225 & -.367 & -.093 & .019 & .035 & .008 & .074 & -1.000 & .000 \\ .019 & .035 & .008 & -.225 & -.367 & -.093 & -.074 & .000 & -1.000 \end{bmatrix}$$

Case C_5 from Table I

$$\begin{bmatrix} -.291 & -.499 & -.125 & .067 & .110 & .026 & .229 & -.308 & .000 \\ .067 & .110 & .026 & -.291 & -.499 & -.125 & -.229 & .000 & -.308 \end{bmatrix}$$

Case C_6 from Table I

$$\begin{bmatrix} -.086 & -.158 & -.041 & .011 & .024 & .006 & .062 & -.314 & .000 \\ .011 & .024 & .006 & -.086 & -.158 & -.041 & -.062 & .000 & -.314 \end{bmatrix}$$

Case C_7 from Table I

$$\begin{bmatrix} -.439 & -.601 & -.559 & .065 & .110 & .019 & .446 & -1.000 & .000 \\ .065 & .110 & .019 & -.439 & -.601 & -.559 & -.446 & .000 & -1.000 \end{bmatrix}$$

Case C_8 from Table I

$$\begin{bmatrix} -.446 & -.240 & -1.585 & .014 & .050 & .005 & .920 & -1.000 & .000 \\ .014 & .050 & .005 & -.446 & -.240 & -1.585 & -.920 & .000 & -1.000 \end{bmatrix}$$

Case C_9 from Table I

$$\begin{bmatrix} -.439 & -.199 & -2.465 & -.031 & -.034 & -.003 & 1.179 & -1.000 & .000 \\ -.031 & -.034 & -.003 & -.439 & -.199 & -2.465 & -1.179 & .000 & -1.000 \end{bmatrix}$$

From Table II with the Bias = $\frac{1}{2}\beta_{a1}$ for normal operation

$$\begin{bmatrix} -.262 & -.425 & -.107 & .125 & .186 & .045 & -.139 & -1.000 & .000 \\ .125 & .186 & .045 & -.262 & -.425 & -.107 & .139 & .000 & -1.000 \end{bmatrix}$$

From Table II with the Bias = $2\beta_{a1}$ for normal operation

$$\begin{bmatrix} -.828 & -1.155 & -.271 & .007 & .034 & .007 & .824 & -1.000 & .000 \\ .007 & .034 & .007 & -.828 & -1.155 & -.271 & -.824 & .000 & -1.000 \end{bmatrix}$$

Unequal Areas--2 Times

$$\begin{bmatrix} -.423 & -.658 & -.162 & .060 & .091 & .021 & .109 & -1.000 & .029 \\ .609 & .094 & .021 & -.395 & -.617 & -.153 & -.057 & .029 & -1.000 \end{bmatrix}$$

Unequal Areas--4 Times

$$\begin{bmatrix} -.426 & -.661 & -.163 & .051 & .081 & .019 & .074 & -1.000 & -.044 \\ .063 & .085 & .019 & -.379 & -.594 & -.147 & -.017 & .004 & -1.000 \end{bmatrix}$$

Unequal Areas--10 Times

$$\begin{bmatrix} -.429 & -.664 & -.163 & .050 & .076 & .019 & .052 & -1.000 & -.054 \\ .060 & .079 & .018 & -.369 & -.579 & -.144 & -.001 & .054 & -1.000 \end{bmatrix}$$

QV Control for Positive T_i with $\omega_i = 1.$

$$\begin{bmatrix} -.370 & -.579 & -.143 & .054 & .078 & .018 & .151 & -.885 & -.033 \\ .053 & .078 & .018 & -.407 & -.637 & -.157 & -.165 & -.047 & -.977 \\ .079 & .075 & .015 & -.048 & -.043 & -.008 & .072 & .137 & -.063 \\ .024 & .024 & .005 & .007 & .009 & .002 & .010 & .051 & .023 \end{bmatrix}$$

QV Control for Negative T_i with $\omega_i = 1.$

$$\begin{bmatrix} -.338 & -.535 & -.133 & -.030 & -.043 & -.011 & .121 & -.861 & -.191 \\ -.026 & -.042 & -.011 & -.186 & -.291 & -.072 & -.063 & -.140 & -.466 \\ .010 & .122 & .028 & .161 & .144 & .029 & -.092 & .266 & .355 \\ -.291 & -.219 & -.039 & .454 & .358 & .067 & -.617 & -.411 & .788 \end{bmatrix}$$

Infinite Bus Optimization with $T_{12} = .545$

$$\begin{bmatrix} -.433 & -.671 & -.165 & .000 & .000 & .000 & .038 & -1.000 & .000 \\ .000 & .000 & .000 & -.433 & -.671 & -.165 & -.038 & .000 & -1.000 \end{bmatrix}$$

Suboptimal Control with $T_{12} = .545$

$$\begin{bmatrix} -.414 & -.654 & -.141 & .000 & .000 & .000 & .229 & -.993 & .000 \\ .000 & .000 & .000 & -.414 & -.654 & -.141 & -.229 & .000 & -.993 \end{bmatrix}$$

Composite Optimization with $T_{12} = 2.725$

$$\begin{bmatrix} -.507 & -.877 & -.209 & .162 & .331 & .073 & .740 & -1.000 & .000 \\ .162 & .331 & .073 & -.507 & -.877 & -.209 & -.740 & .000 & -1.000 \end{bmatrix}$$

Infinite Bus Optimization $T_{12} = 2.725$

$$\begin{bmatrix} -.605 & -.951 & -.228 & .000 & .000 & .000 & .404 & -1.000 & .000 \\ .000 & .000 & .000 & -.605 & -.951 & -.228 & -.404 & .000 & -1.000 \end{bmatrix}$$

Suboptimal Control with $T_{12} = 2.725$

$$\begin{bmatrix} -.465 & -.821 & -.161 & .000 & .000 & .000 & .791 & -.959 & .000 \\ .000 & .000 & .000 & -.465 & -.821 & -.161 & -.791 & .000 & -.959 \end{bmatrix}$$

VITA

In Beaumont, Texas, on August 4, 1945, the author became the second son of Daniel M. and Evelyn Reddoch Sr. A resident of Beaumont all of his pre-college life, he attended public school in the Beaumont Independent School System. After graduation from Beaumont High School in May 1963, he entered Lamar University in Beaumont to study electrical engineering. He received his B. S. degree in electrical engineering in May 1967 and his Master of Engineering Science degree in February 1969 from Lamar. He received the Doctor of Philosophy degree in electrical engineering from Louisiana State University in May 1973 concentrating in the areas of power systems and automatic control systems.

As an undergraduate he has been affiliated with the honor organization of Eta Kappa Nu, Tau Beta Pi, Phi Kappa Phi, Phi Eta Sigma, and Blue Key as well as the professional organization of IEEE. He has held several elective students offices in Eta Kappa Nu, IEEE, and Phi Eta Sigma. He is currently a member of the Power Engineering Society and the Control Systems Society of IEEE. As a graduate student at Louisiana State University, he published articles in technical journals and has made presentations before national and regional meetings.

The author has held summer positions with several companies. He worked for the Sun Oil Company in Beaumont as an engineer trainee in 1965 and 1966, for the Naval Ordinance Laboratory in Silver Springs, Maryland as an electrical engineeer in 1967, and for Gulf States Utilities in Beaumont as a consultant engineer in 1968 and 1969.

As a graduate student, he held the position of Teaching Fellow of Engineering at Lamar and Shell Fellow and research assistant at Louisiana State University. After completion of the master's degree he taught in the Department of Electrical Engineering of Lamar as an instructor. Effective March 1, 1973, he became an assistant professor with the Department of Electrical Engineering at the University of Tennessee at Knoxville.

EXAMINATION AND THESIS REPORT

Candidate: Thomas William Reddoch

Major Field: Electrical Engineering

Title of Thesis: Models and Cost Functionals for Optimal Automatic Generation Controllers

Approved:

Paul M. Julich
Major Professor and Chairman

Max Goodrich
Dean of the Graduate School

EXAMINING COMMITTEE:

Marion E. Council

Owen T. Tan

Edgar C. Tucker

Dan R. Scholz

Date of Examination:

February 28, 1973